Chapter 1

Introduction

1 Introduction

1.1 Bioenergy and biofuels

Bioenergy and biomass are sustainable forms of renewable energy available for commercial use and have been well-utilized for transport as well as industry needs (Stančin et al., 2020). According to International Energy Agency (IEA) in 2018, bioenergy is the largest contributor to the world's energy needs, accounting for 53% of the total renewables (Kumar et al., 2020). Bioenergy includes biofuels like biodiesel or bioethanol (used for transportation), biomass like wood chips or pellets (used as feed, fodder, or to produce electricity and heat), and biogas like biomethane or biohydrogen obtained from waste material (IEA, 2013) (Ho et al., 2014a). Biofuels have evolved into four generations based on the feedstock (**Figure 1.1**). The first-generation biofuels are derived from edible feedstocks and their prolonged use negatively impacts both the economy and the environment (Ho et al., 2014a; Mat Aron et al., 2020; Datta et al., 2019). Second-generation biofuels were born from non-edible feedstocks and their energy efficiency is also high. However, the fuel extraction steps are energy-intensive (Lee and Lavoie, 2013) which contributed to the emergence of third-generation microalgal sources. The third-generation sources generate environment-friendly, high-yielding biofuel with minimum land area needed for cultivation (Kumar et al., 2013).

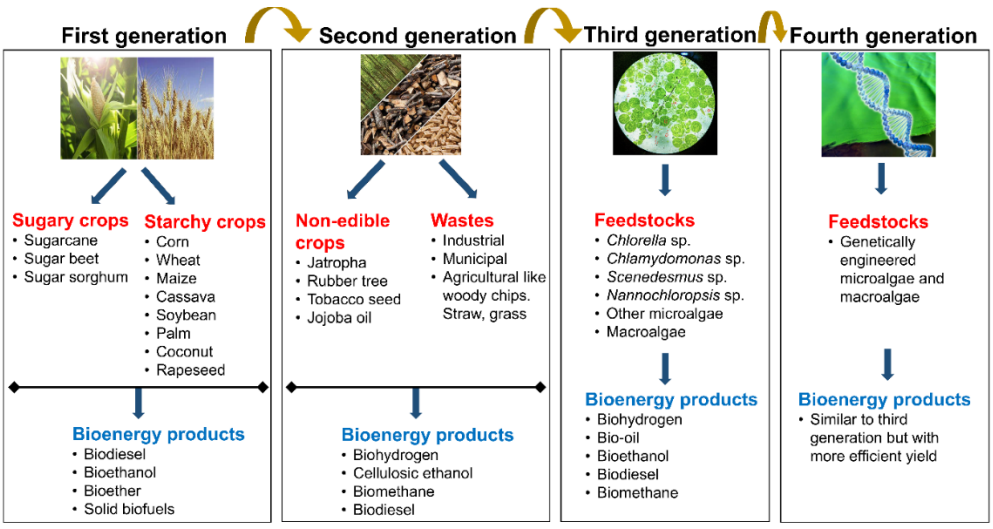

Figure 1.1. Four generations of biofuel as based on the feedstock used for biofuel production.

1.2 Microalgae as the prominent source of biofuel and nutraceuticals

Microalgal sources offer high lipid/oil content, increased oil yield, less use of land, and hence the highest biodiesel productivity. Microalgae are capable of harnessing solar energy as well as fixing atmospheric carbon dioxide. They possess a faster growth rate, thus reducing the cost of cultivation (Udayan et al., 2022). Microalgae-based biodiesel has properties like density, viscosity, flash point, heating point, and cold filter plugging point similar to petroleum diesel and meets the standards of both the American Society for Testing and Materials (ASTM) and the International Biodiesel Standard for Vehicles (Alalwan et al., 2019). The net production per acre area of microalgal bioethanol is almost 15 times higher than that obtained from corn and undergoes minimum pre-treatment steps for final production. Microalgae-based bio-oil has a high heating value, low density, and low viscosity compared with fossil-based oil produced from wood and also has better quality (Alalwan et al., 2019). In addition to the production of biodiesel, bioethanol, and bio-oil, microalgal biomass has wide applications in wastewater treatment, the synthesis of carotenoids, agar, antioxidants, and catalysts, in cosmetics, pharmaceutics, and therapeutics (Dębowski et al., 2020).

Microalgae are unicellular micro-organisms broadly divided into four classes: (i) *Cyanobacteria* (blue-green algae), (ii) *Rhodophytes* (red algae), (iii) *Chlorophytes* (green algae), and (iv) *Chromophytes* (all other algae) (Mobin and Alam, 2017) (**Figure 1.2**). *Spirulina*, blue-green algae, also categorized as "Super Natural Food", is rich in proteins, vitamins, essential polyunsaturated fatty acids (PUFA), photosynthetic pigments, and minerals. It serves as a commercial source of phycocyanin pigments (Costa et al., 2019). Green microalgae include *Dunaliella*, *Chlorella*, *Scenedesmus*, *Chlamydomonas*, etc. *Chlorella* is a rich source of several vitamins like Vit. E, B-complex, provitamin A, and β-carotene and has over a billion US dollars in commercial value. It is one of the most widely used commercial microalgae in biodiesel production (Mobin and Alam, 2017). *Scenedesmus* is capable of producing lipid content varying between 10 to 50 % of its dry weight and can be effective in wastewater treatment and other bioremediation purposes (Msanne et al., 2020). In a vegetative cell of photoautotrophically cultivated *Chlamydomonas reinhardtii*, carbohydrates constitute a major portion of the cell's dry weight which is 52%, followed by 27% proteins, 19% lipids, and only 2% chlorophyll (Li-Beisson et al., 2015).

Table 1.1 highlights biofuel production and pharmaceutical and nutraceutical applications of a few microalgal species.

Microalgae serves as a potent competitor to edible and non-edible crops for biofuel generation. However, there are certain limitations. Even though the process is capable of fixing the greenhouse gases from the atmosphere, reports claim that it releases more greenhouse gas into the atmosphere than it fixes (Mat Aron et al., 2020). Also, the amount of energy lost or used in the process is more than the energy produced, resulting in net negative energy gain (Mat Aron et al., 2020). Other than water, the cultivation of microalgae also depends on the availability of nutrients like nitrogen, sulfur, or phosphorous (Datta et al., 2019). The fourth-generation biofuel was introduced to increase the energy supply and decrease the cost of biofuel production. Here, the feedstocks are genetically modified microalgae. These microorganisms are modified to increase the intake of CO_2 for photosynthesis, creating an artificial carbon sink and enhancing the production of biofuel. Many algal strains (eg. *Chlamydomonas reinhardtii*, *Phaeodactylum tricornutum*, etc.) have been genetically modified to increase the growth rate and adaptability to grow in poor nutrient environments. For example, overexpressing malonyl-CoA acyl-carrier protein transacylase in *Nannochloropsis oceanica* resulted in an increase in the neutral lipid content by 31% (Chen et al., 2017b). Overexpression of *ACS2* (acetyl-CoA synthetase gene) in *Chlamydomonas reinhardtii* increases the lipid content by 2.4-folds under nitrogen starvation (Rengel et al., 2018). Similar genetic engineering of *C. reinhardtii* with genes involved in *de novo* lipid production pathways enhances the lipid content by 5-8 times with an increase in the long-chain saturated and monounsaturated fatty acid content (Wang et al., 2017). The fourth generation of biofuels also involves methods and technologies like pyrolysis (in a temperature range between 400 to 600℃) and gasification (Alalwan et al., 2019). However, the knowledge about fourth-generation biofuel production is only limited as it started in the year 2006 and so is in the early development stage (Datta et al., 2019).

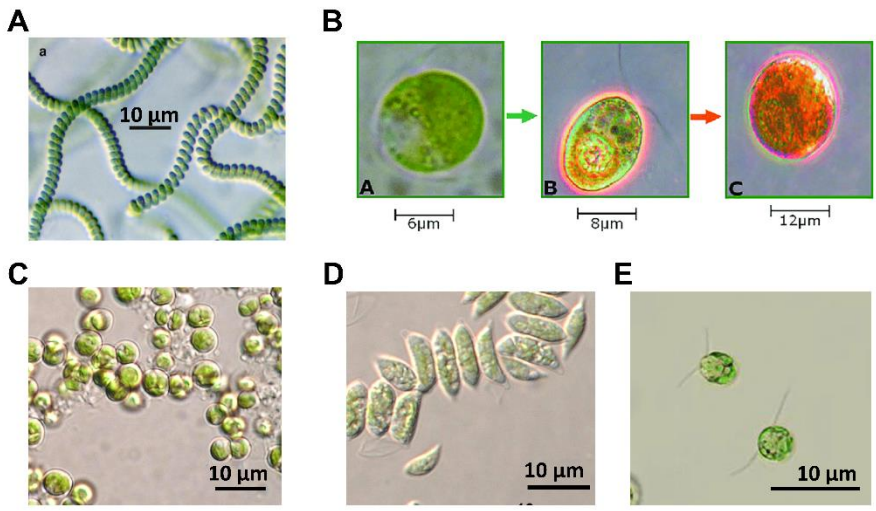

Figure 1.2. Microscopic images of microalgae involved in biofuel production.

A. Clonal trichomes of *Spirulina subsalsa* (*Arthrospira* sp.) (Whitton, 2012). **B**. Advancing stages of *Dunaliella salina* under saline stress with increasing time of incubation, cells appear swollen due to osmotic imbalance at the stationary phase of the growth cycle (C) as opposed to the early logarithmic phase in (A) (Gallego-Cartagena et al., 2019). **C** and **D**. Cells of *Chlorella* sp. and *Scenedesmus* sp. under optimum growth conditions (Source: Culture Collection of Autotrophic Organisms). **E**. Oval-shaped cells of *Chlamydomonas reinhardtii* with two anterior flagella (Source: UTEX, https://utex.org/products/utex-0089).

Table 1.1. Biofuel production, pharmaceutical, and nutraceutical application of a few microalgal species

Microalgal species	Bioproduct	Application	References
Chlorella sp.	Chlorophyll	Food additives, anti-oxidant	(Khanra et al., 2018)
Dunaliella tertiolecta	Carotenoid (Violaxanthin)	Anti-neoplastic activity	(Tang et al., 2020)
Dunaliella salina	Carotenoid (β-carotene)	Anti-oxidants	(Xu et al., 2018)
Haematococcus pluvialis, Chlorella vulgaris	Carotenoid (Astaxanthin)	Anti-inflammatory and anti-apoptotic properties	(Khoo et al., 2019)
Chlorella sorokiniana	Carotenoid (Lutein)	Anti-oxidant	(Ma et al., 2020)
Phaeodactylum tricornutum, Chlamydomonas nivalis	Carotenoids (Fucoxanthin and Zeaxanthin)	Anti-cancer, anti-diabetic	(Gong and Bassi, 2016)
Spirulina platensis	Phycobiliproteins carotenoids, biomass	Pigments, cosmetics, pro-vitamins	(Li et al., 2008)
Chlorella vulgaris, Nannochloropsis sp.	PUFA (Eicosapentaenoic acid, EPA)	Blood clotting, coronary heart disease	(Levasseur et al., 2020)
Crypthecodiuimu sp., *Schizochytrium* sp.,	PUFA (Docosahexaeonic acid, DHA)	Anti-inflammatory, anti-cancer	(Long et al., 2018)
Spirulina platensis	Fatty acid (γ-linolenic acid, GLA)	Nutritional supplement	(Sajilata et al., 2008)
Scenedesmus sp., *Acutodesmus* sp., *Chlorella* sp.	Neutral lipid	Biodiesel, transportation, power plant	(Chokshi et al., 2015; Pancha et al., 2015b; Bhattacharya et al., 2016)

1.3Factors influencing the biofuel production in microalgae

Altering the cultivation strategies impact the biofuel content. The presence of abiotic stress element in the culture environment becomes an important governing factor in biofuel production. Altogether, these elements further influence biofuel quality. The factors involved in biofuel manipulation in microalgae are summarized in **Figure 1.3**.

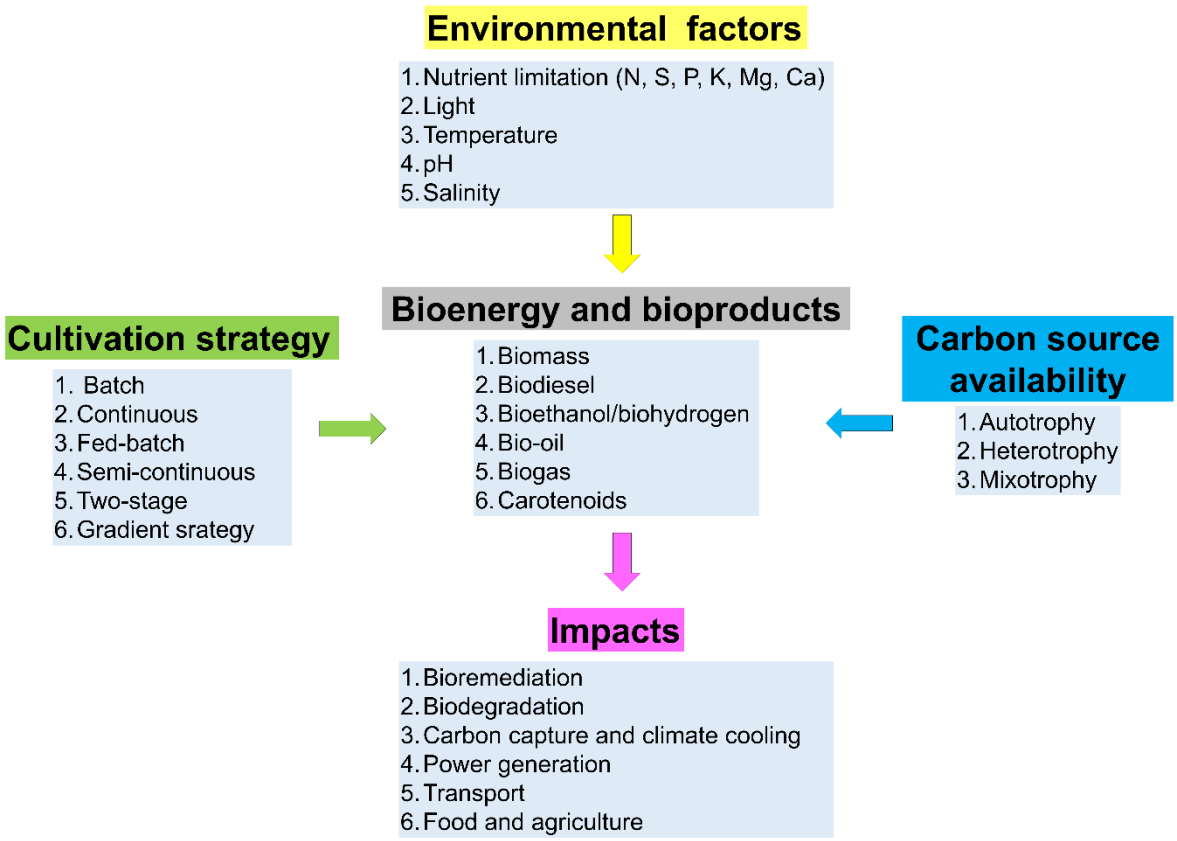

Figure 1.3. Factors governing biofuel production in microalgae and their impact on the environment and society.

1.3.1 Environmental factors

1.3.1.1 Nutrient manipulation

Depleting or limiting microalgal growth medium of essential nutrients like nitrogen, phosphorous, sulfur, magnesium, and calcium causes a trade-off between the growth and production of storage metabolites like carbohydrates and lipids (Ran et al., 2019). N depletion has shown more adverse effects on growth and photosynthesis than N limitation (Benavente-Valdés et al., 2016). N limitation in *Nannochloropsis gaditana* has been revealed to increase carbohydrate and lipid production as compared to N depletion (Heredia et al., 2021). To overcome the stressful effect of N depletion, stepwise nitrogen depletion in *Chlorella vulgaris* has been shown to improve the growth rate and the carotenoid content (Zhang et al., 2017). Under P limitation, the triose phosphate-Pi exchange is hampered resulting in the excess of triose phosphate in chloroplast which provides the substrate for starch production (Ran et al., 2019; Paliwal et al., 2017). Compared to N limitation, P limitation has caused higher lipid concentration in *C. reinhardtii* due to better photosynthetic efficiency and protein content (Chen and Wang, 2021). Microalgae consortia have shown higher starch and lipid content under N limitation and high protein content under phosphorous limitation (Phalanisong et al., 2021). S depletion resulted in increased starch and lipid accumulation, better than N or P depletion, as observed in *Chlamydomonas reinhardtii* and *Chlorella vulgaris* (Cakmak et al., 2012; Ran et al., 2019).

1.3.1.2 Light

Altering light intensity, duration, photoperiod, and wavelength impacts photosynthesis and microalgal growth. Low light intensity induces the formation of membrane polar lipids, while high light intensity increases the production of neutral lipids like TAG along with a concomitant decrease in PUFAs (Chen and Wang, 2021; Paliwal et al., 2017). High light intensity results in photoinhibition and ROS production causing photooxidative damage to biomolecules and cell death (Erickson et al., 2015). A microalgal polyculture exposed to high light resulted in high lipid content, while low light caused high biomass accumulation (Iasimone et al., 2018). Photoperiod also governs the PUFA content. In a study on *C. vulgaris*, 16:8 h light: dark induces more

SFAs while 8:16h causes more PUFA accumulation (Khoeyi et al., 2012). The ideal photoperiod varies among different microalgae (Smith and Gilmour, 2018).

1.3.1.3 Temperature

Temperature imposes a direct effect on membrane fluidity and the total lipid content of microalgae. Low temperatures result in the accumulation of polar lipids like PUFAs, while higher temperatures induce neutral lipid formation (Paliwal et al., 2017). PUFAs directly regulate the membrane fluidity and act as a cryoprotectant (Chen et al., 2017a). For example, in *Acutodesmus dimorphus*, temperature stress at 35 ℃ results in increased total lipid content to 22.7% and neutral lipid to 59% of total lipid content (Chokshi et al., 2015). Prolonged exposure to low-temperature stress can result in oxidative damage, chlorosis, and decreased growth rate, which eventually leads to cell death (Valledor et al., 2013). Similarly, prolonged high-temperature stress affects protein folding, membrane fluidity, metabolism, DNA replication, and repair, ultimately resulting in cell death. In *Chlamydomonas*, the optimum temperature ranges between 20-25 ℃, and heat shock response is activated when shifted to at least 37 ℃ and gets fatal beyond 42 ℃ (Schroda et al., 2015).

1.3.1.4 Salinity

Salinity stress imposes maximum lipid production compared to the other stress-inducing factors. The increase in Na^+ and Cl^- concentration in the culture medium causes an osmotic imbalance across the cell membrane resulting in osmotic stress (Benavente-Valdés et al., 2016). The osmoprotectants like glycerol and ROS molecules help the cell overcome such stress. ROS production is known to activate autophagy-induced lipid and carotenoid production (Perez-Perez et al., 2012). However, high salt concentrations also result in compromised photosynthetic efficiency and cell death as salinity stress hampers cell size and cell division. In freshwater *Chlamydomonas* sp., a characteristic type of "palmelloid" formation is observed, where the cell wall thickens and the clusters of two or more cells are surrounded by an exopolysaccharide layer which provides them protection (**Figure 1.4**) (Shetty et al., 2019). Salt-tolerant species like those surviving in seawater, for example, *Chlamydomonas* sp. JSC4 possesses the machinery to overcome the negative effects of salt-induced osmotic shock and hence

can offer increased lipid production at the cost of minimum compromise to growth (Ho et al., 2014b).

1.3.1.5 Others

pH values can also alter lipid production in microalgae (Chen et al., 2017a). An alkaline pH (>9) along with nitrogen limitation and salinity stress increases the TAG accumulation in *Scenedesmus* sp (Gardner et al., 2011). Incrementing pH change in the culture medium results in enhanced TAG accumulation than the constant pH stress, as observed in a few *Chlorellaceae* strains (Skrupski et al., 2013). Brefeldin A treatment increases the TAG accumulation in *C. reinhardtii* and *C. vulgaris* by inducing ER stress (Kim et al., 2013). Sodium azide leads to growth retardation and inhibition of photosynthesis and respiration resulting in a 60-80% increase in TAG content in *Chlorella desiccate* (Rachutin Zalogin and Pick, 2014). The use of phytohormones like auxin has been shown to enhance growth and lipid production in *Scenedesmus* sp. (Dao et al., 2018).

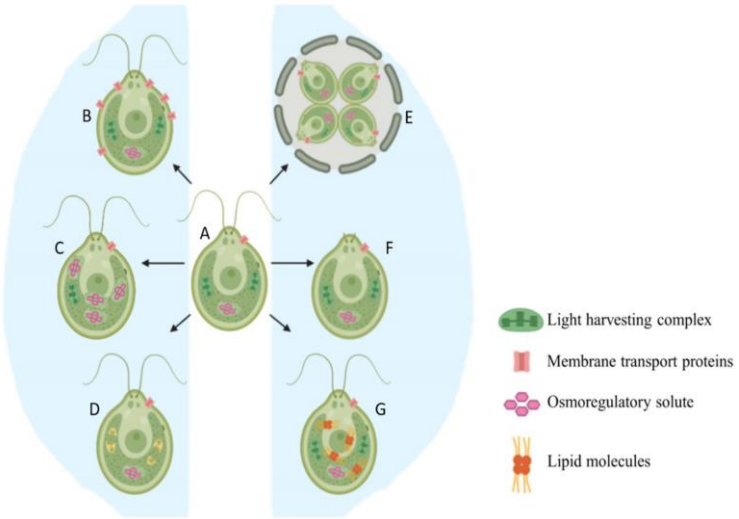

Figure 1.4. A model representing morphological changes in *Chlamydomonas* sp. under saline stress.

A microalgal cell under no stress (A) undergoes a series of events (B-G) under saline stress where membrane transport proteins are upregulated (B), osmoregulating solutes like glycerol accumulates (C), light-harvesting complexes start to degrade (D), palmelloid is formed (E), cells lose their flagella and motility (F), and finally, lipid accumulation is observed (G) (Shetty et al., 2019) (See Appendix A6.1. for copyright information).

1.3.2 Carbon source availability

Carbon forms another important element used by microalgae for biomass production. The use of sunlight with atmospheric CO_2 as the carbon source forms the most widely used cultivation method for the growth of microalgae in industries and research labs, except for *Crypthecodinium cohnii* which is a strict heterotroph (Saha and Murray, 2018). Apart from the usual photoautotrophy mode, the majority of the microalgae can also generate energy from heterotrophic and mixotrophic modes of cultivation.

1.3.2.1 Photoautotrophic cultivation

Phototrophy or autotrophy is the most common and the easiest method of cultivation of microalgae. The ability to fix atmospheric carbon dioxide allows photoautotrophs to contribute to easy greenhouse gas mitigation along with the efficient removal of N and P from the atmosphere (Abdel-Raouf et al., 2012). A CO_2 level of 2% is the optimum concentration to enhance biomass production in microalgae (Sajjadi et al., 2018). Low CO_2 levels (less than 2%) have been found to produce more unsaturated fatty acids while 2-10% CO_2 causes reduced unsaturation content in the fatty acids of microalgae (Cheng and He, 2014). Moreover, high CO_2 levels can disturb the pH of the medium. In such a case, the addition of sodium bicarbonate in the medium acts as a buffer with excellent solubility in water (Ran et al., 2019). Bicarbonate at 0.6 g/l was found to be optimum in *Scenedesmus* sp. for lipid, carbohydrate, and biomass production (Pancha et al., 2015a). Autotrophic cultivation also features the production of the maximum carbohydrate content in microalgae (Puzanskiy et al., 2021). Autotrophy serves as the control method for growth-related experiments. However, compared to heterotrophic and mixotrophic cultivation, it produces low biomass concentrations, giving rise to poor productivity (Patel et al., 2020). As a result, the research nowadays is focussed on introducing biomass-elevating components to the autotrophic cultivation like, the organic carbon sources (Lin and Wu, 2015).

1.3.2.2 Heterotrophic cultivation

Glucose is the most commonly used external energy source in microalgae (Perez-Garcia et al., 2011) for its ability to yield higher energy than acetate or fructose (Boyle and Morgan, 2009). *Chlorella protothecoids* when grown heterotrophically on glucose yield

260% more lipids compared to autotrophic growth (Miao and Wu, 2006). Heterotrophic growth is not limited to only glucose. The presence of acetate and glycerol as the carbon source also improved the cell density and lipid productivity of *Chlorella vulgaris* (Liang et al., 2009). The increase in lipid productivity is doubled in *Chlorella protothecoids* in presence of glycerol (Chen and Walker, 2011). Moreover, the production cost is decreased by ~80% as compared to glucose (Wang et al., 2016). *Chrypthecodinium cohnii*, an obligatory heterotroph is capable of growing on wastes with high COD demands and producing valuable products like DHA (Mendes et al., 2007). *Chlorella* sp. and *Scenedesmus* sp. have been grown successfully on acid-rich effluent and efficiently delivered biomass and lipids (Prathima Devi et al., 2012). However, the presence of the organic carbon source increases the risk of culture contamination and CO_2 emissions (da Silva et al., 2021).

1.3.2.3 Mixotrophic cultivation

Cyanobacteria and green algae like *Chlorella vulgaris*, *Spirulina platensis*, *Haematococcus pluvialis*, and *Euglena gracilis* can efficiently grow in a mixotrophic mode as compared to the other two modes (Perez-Garcia and Bashan, 2015). Here, photosynthesis takes place by fixing the light in the light phase of the growth, and aerobic respiration uses the organic carbon source in the dark phase of growth. (Wang et al., 2014a). Mixotrophic cultivation causes an extended exponential phase, hence higher biomass yield and increased lipid productivity. For example, the mixotrophic regime with glucose in *Nannochloropsis oculata* and *Chlorella sorokiniana* show 2 to 4 times improved biomass over photoautotrophy (Wan et al., 2011). The use of organic carbon sources like glucose, sucrose, xylose, and acetate in mixotrophic modes of cultivation further increases lipid production in *Chlorella vulgaris* (Lin and Wu, 2015). The lipid productivity is increased by ~10 times in *Chlorella vulgaris* in presence of glucose (Liang et al., 2009). Mixotrophy also improves the bioproduct formation when combined with bioremediation. *C. vulgaris* grown mixotrophically on orange peel extracts yields ~3 times more biomass and ~4 times more lipids than glucose-containing medium (Park et al., 2014). Mixotrophic *C. vulgaris* also produce maximum biomass and lipids when grown on chicken wastes used as a nutrient source (Tan et al., 2021). Mixotrophy reduces CO_2 emissions by ~60% in *Chlorella protothecoids* (Xiong et al.,

2010). However, the risk of contamination still exists along with the chances of photoinhibition at higher carbon concentrations (Patel et al., 2020).

1.3.3 Cultivation strategy

1.3.3.1 Batch cultivation

Here, a fixed amount of microalgal cells are inoculated into the fully enriched culture medium in a reactor. The cells continue to divide only until the medium supplements sustain, and hence follow a sigmoidal growth pattern (Ganesan et al., 2020). Although the easiest operation strategy, it limits biomass production and hence lipid productivity, as observed in *Acutodesmus obliquus* and *Nannochloropsis* sp. under lab-scale batch nitrogen starvation (Remmers et al., 2017; Benvenuti et al., 2016).

1.3.3.2 Continuous flow cultivation

Here, a certain amount of nutrient-rich fresh medium is continuously introduced into the reactor and the division of microalgal cells never tends to cease. The growth of microalgal cells attains a steady state, where the birth rate is equivalent to the death rate. Turbidostat and chemostat are two types of steady states. Turbidostat is attained when the fresh medium is added after the cells have reached a certain limit, while chemostat culture is accomplished when the fresh medium is introduced at a predetermined state (Ganesan et al., 2020). The continuous flow strategy is seldom practiced commercially since the ratio of medium feeding is a critical parameter to control (Wang et al., 2014a). The continuous flow method is always better to increase the bioenergy yield. Continuous culture of *C. reinhardtii* has been shown to produce improved yields of biohydrogen than it does in batch mode (Das et al., 2015). In another independent study, the selection of chemostat mode over batch mode resulted in better yields of lipids and carbohydrates in *Nannochloropsis gaditana* under nitrogen limitation (Heredia et al., 2021).

1.3.3.3 Fed-batch cultivation

Unlike the continuous mode of operation, in fed-batch culture, a small but fixed amount of fresh nutrient-rich medium is intermittently added to the reactor. This kind of strategy

does not restrict the substrate availability and results in a higher growth rate and lipid productivity as compared to the batch culture (Wang et al., 2014a). Mixotrophic fed-batch cultivation of *C. reinhardtii* amplified the cell density and production of osmoregulatory molecules (Fields et al., 2018). In *C. protothecoides*, oxygen and nitrogen limitations in fed-batch cultivation increased lipid productivity, and N-limitation and temperature stress caused higher lutein content (Chen et al., 2017a).

1.3.3.4 Semi-continuous cultivation

This is a modified culture strategy where the fresh medium is first supplied altogether to the culture and is allowed to grow for a fixed time, after which a certain volume of culture is withdrawn at fixed time intervals and the volume is replenished by the fresh nutrient-rich medium. This allows mature cells to continuously divide and they never face substrate restriction. Semi-continuous mode offers better growth rates but lower lipid productivity than batch culture (Benvenuti et al., 2016). Open pond cultivation of cyanobacterium, *Anabaena* sp., in semi-continuous mode proved beneficial for biomass production (Veerabadhran et al., 2021).

1.3.3.5 Two-stage cultivation

In the two-stage, a combination of two operation strategies is combined (Liyanaarachchi et al., 2021). Often, there exists a vegetative stage where the cells are allowed to flourish under optimum growth conditions, followed by stress where stress factors like nutrient limitations or environmental changes induce biofuel production. For instance, auxin addition in the first stage followed by salinity stress in the second stage in *Dunaliella tertiolecta* caused a tremendous increase in the lipid content from 24% to 70% (Aziz et al., 2020). It also benefits carotenoid and chlorophyll production (Liyanaarachchi et al., 2021). Two-stage cultivation of *Chlorella vulgaris* under salt and light stress enhanced the carotenoid production along with biomass and lipid content (Ali et al., 2021). In another independent study, the mixotrophic stage followed by the photoautotrophic stress imposed stage in *C. vulgaris* improved lipid productivity (Wensel et al., 2022). Similarly, two-stage cultivation of *Botryococcus braunii* caused a marked increase in biofuel production to one-stage (Thurakit et al., 2022).

1.3.3.6 Gradient strategy of cultivation

Here, a stepwise increase of stress factors induces acclimation of the microalgae to stress factors. As a result, biomass yield is improved more than that obtained in two-stage. Step-wise addition of multiple stresses (salinity, light, and temperature) to *Scenedesmus* sp. resulted in multiple tolerance and the highest lipid content (Maneechote and Cheirsilp, 2021). Salinity gradient in salt-tolerant *Chlamydomonas* sp. JSC4 has improved lipid productivity (Ho et al., 2014b) and also increased the lutein content along with biomass yield (Xie et al., 2019). Similarly, the stepwise addition of salt to the halophilic strain of *Dunaliella salina* culture markedly increased biomass and lipid productivity (Abomohra et al., 2020). High light intensity causes damage to the *Aurantiochytrium* sp, hence, sequentially applying a light gradient solves the problem of cell damage and also improves the DHA and total oil yield (Yin et al., 2022).

Some of the recently used strategies to improve the yield of bioenergy are shown in **Table 1.2**.

Table 1.2. Recent advances to improve the bioenergy yield in microalgae

Microalgal species	Yield/productivity of bioproduct	Cultivation strategy	References
Dunaliella salina KSA-HS022	Biomass productivity- 0.191 g L^{-1} d^{-1} Lipid productivity- 56.5 mg L^{-1} d^{-1}	Stepwise salinity stress	(Abomohra et al., 2020)
Chlorella zofingiensis	Cell density- 8.37 × 10^7 ± 3.65 × 10^6 cells/mL Lipid productivity- 0.027 ± 0.002 g L^{-1} d^{-1} Total carotenoids- 0.85 ± 0.03 % DW	Two-stage batch cultivation with acetate supplementation and urea as the nitrogen source	(Minyuk et al., 2020)
Chlorella sorokiniana MB-1-M12	Biomass productivity- 1.074 ± 0.020 g L^{-1} d^{-1} Lutein productivity- 4.50 ± 0.08 mg L^{-1} d^{-1}	Two-stage heterotrophic-mixotrophic (TSHM) process resulted	(Chen et al., 2021)
Chlorella vulgaris	SFA content increased by 27.3%	Two-stage strategy- the first stage includes wastewater and the second stage includes nitrogen and salt stress	(Mirizadeh et al., 2020)
Scenedesmus SDEC-8, *Chlorella sorokiniana* SDEC-18	Lipid productivity- SDEC-8: 26.7 mg/L/d, SDEC-18: 25.9 mg/L/d	Phytohormone addition coupled with nitrogen depletion	(Yu et al., 2018)
Chlorella pyrenoidosa	Total lipid content- 18.53% DW	Heterotrophic cultivation on furfural wastewater	(Cheng et al., 2022)
Scenedesmus obliquus	Lipid productivity- 18.77 ± 0.07 mg L^{-1} d^{-1}	Fe_2O_3 nanoparticles	(He et al., 2017a)
Chlamydomonas reinhardtii	47-fold higher zeaxanthin productivity	Genetic modification using CRISPR/Cas9 technology	(Baek et al., 2018)

1.4 Metabolite synthesis pathways and their regulation in microalgae

Among all the metabolites synthesized by the microalgae, the important ones in biofuel research are lipids, carbohydrates especially starch, and photosynthetic pigments i.e. chlorophyll and carotenoids. Lipids are processed to produce biodiesel, downstream processing of starch generates biohydrogen and bioethanol, carotenoids are used in nutraceuticals, and along with chlorophyll they form an essential component of many pharmaceuticals and pharmacological products (as discussed in **Table 1.1**). Hence, to upgrade their production it becomes important to understand the biochemical pathways involved in their synthesis and regulatory networks.

1.4.1 Starch metabolism

Carbohydrates are the energy reserves produced by photosynthesis and starch is the primary energy sink in microalgae. In green microalgae, starch is synthesized in chloroplast using ADP-glucose as the glucose donor, while in red algae and dinoflagellates, starch is synthesized in cytosol using UDP-glucose as the donor (de Carvalho Silvello et al., 2022; Ran et al., 2019). Green microalgae can synthesize starch for up to 50% of its dry weight and the concentration changes upon manipulating environmental conditions like nitrogen starvation (Levasseur et al., 2020).

The classic starch biosynthetic pathway in microalgae is demonstrated in **Figure 1.5.** Starch is primarily synthesized around the pyrenoids in *Chlamydomonas*, however high light intensities and increased CO_2 levels can cause the excess starch to accumulate in the stroma. The biosynthesis in *C. reinhardtii* is limited by the catalytic conversion of glucose to ADP-glucose by ADP-glucose pyrophosphorylase (AGPase) (Ball, 2002). The AGPase is activated by 3-PGA (the first product of the Calvin-Benson cycle) and allosterically inhibited by the inorganic phosphate molecules (Ball and Deschamps, 2009; Li et al., 2011). Starch accumulation under high phosphate levels is attributed to the activity of the starch phosphorylase (SP) enzyme which catalyzes starch degradation by reversibly converting α-1,4-glucan and inorganic phosphate (Pi) to glucose-1-phosphate (Yao et al., 2018). Amylases are other starch-degrading enzymes that regulate starch concentration (Busi et al., 2014). AGPase and SP share the same substrate, glucose-1-phosphate, due to which they cannot work efficiently at the same time (Ran et al., 2019). AGPase is further upregulated at the transcription level under

nitrogen-depleting conditions (Blaby et al., 2013). The deletion of the gene encoding AGPase (*sta6*) in *C. reinhardtii* induces oxidative stress and autophagic activities (Tran et al., 2019a) and diverts the carbon pool towards lipid accumulation in presence of external carbon sources like acetate (Goodenough et al., 2014).

When *Chlamydomonas* cells are grown in dark aerobic conditions containing acetate, the conversion of acetate to acetyl-CoA followed by glucose synthesis takes place through the gluconeogenesis pathway (Johnson and Alric, 2013). Under anoxic or ATP-deficient conditions, starch gets hydrolyzed to yield glucose molecules by the process called the "Pasteur effect". Here, hexokinase (HK) and phosphofructokinase (PFK) are inhibited and the equilibrium between fructose-1,6-bisphosphate and fructose-6-phosphate shifts towards the bisphosphate and starch synthesis is compromised (Johnson and Alric, 2013).

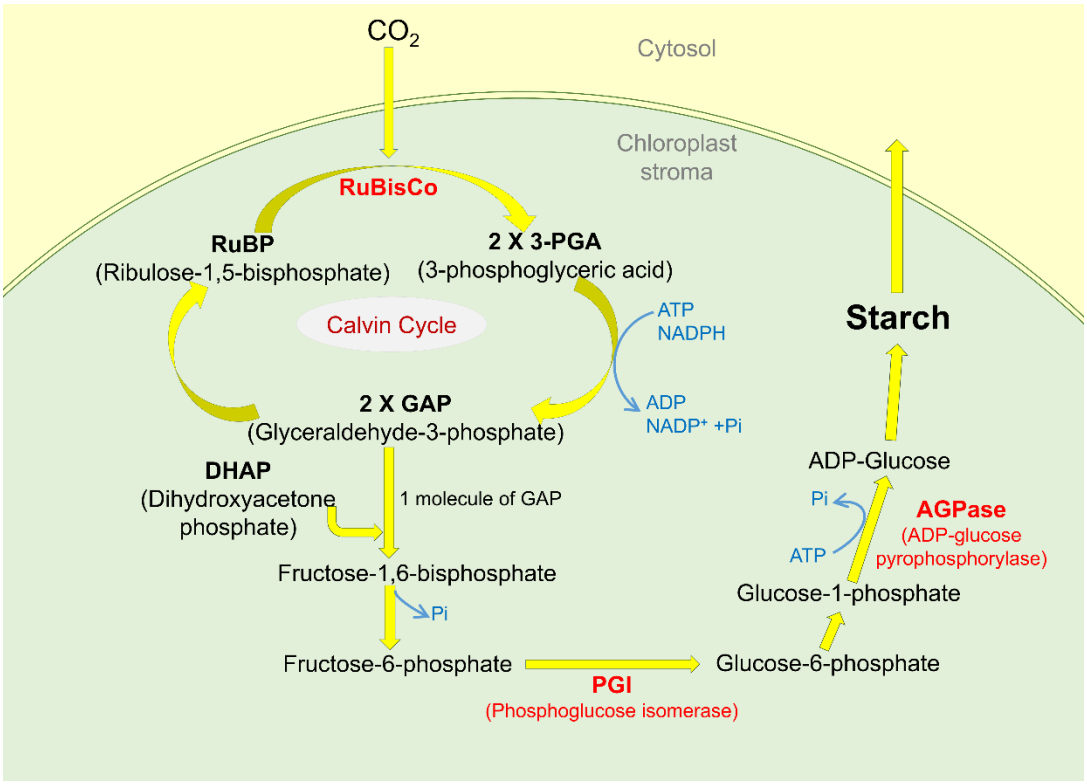

Figure 1.5. Starch metabolism in microalgae

1.4.2 Lipid metabolism

Triacylglycerols (TAGs) are harvested and processed downstream to obtain biodiesel. The length of the carbon chain and unsaturation content of FA constituting TAGs can vary from one microalgal specie to another and also varies under different environmental conditions (Calixto et al., 2018). Microalgae can synthesize neutral lipids constituting up to 20-50% of the cell's dry weight under an abiotic stress environment (Chen and Wang, 2021). Other than biodiesel, polyunsaturated fatty acids like DHA and EPA with pharmaceutical value can also be harvested from these storage lipids (Levasseur et al., 2020).

1.4.2.1 TAG biosynthesis and lipid droplet formation

TAG biosynthesis consists of three basic steps: (1) FA biosynthesis, (2) formation of glycerolipids, and (3) lipid droplet biogenesis. The steps involved in TAG biosynthesis in microalgae are demonstrated in **Figure 1.6.** FA synthesis in green microalgae takes place in the chloroplast, where the conversion of acetyl-CoA to malonyl-CoA catalyzed by acetyl-CoA carboxylase (ACC) forms the rate-limiting step (Liu and Benning, 2013). Acetyl-CoA can be produced directly from acetate supplied externally. When glucose or glycerol is available as the carbon source, glycerol-3-phosphate is produced first which is later enzymatically converted to acetyl-CoA (Chen and Wang, 2021). Glycerol-3-phosphate is the most important intermediate that can also be obtained after the dehydrogenation of DHAP (product of Calvin cycle, **Figure 1.5**) by glycerol-3-phosphate dehydrogenase (GPDH) (Li-Beisson et al., 2019). GPDH in *Chlamydomonas* is upregulated under nitrogen starvation and has two associated activities. It can act as reductases to form glycerol-3-phosphate back from DHAP or phosphatases that form glycerol, depending on the environmental cue (Morales-Sanchez et al., 2017). Salt stress in *C. reinhardtii* increases lipid production and it has been directly co-related to the increased transcript levels of *ACC* (Atikij et al., 2019). Overexpressing gene for the enzyme catalyzing the conversion of malonyl-CoA to malonyl-CoA ACP in *Nannochloropsis* sp. increases the net lipid content by nearly 30% (Chen et al., 2017b). Generally, *C. reinhardtii* produces FAs with C16 to C18 carbon length which can further undergo elongation and desaturation to yield valuable FAs like Δ4 and Δ5 unsaturated PUFA (Li-Beisson et al., 2015).

In *Chlamydomonas*, TAG is synthesized from DAG (diacylglycerols) in the endoplasmic reticulum (ER) and the TAG molecules are transferred to cytosol in the form of lipid droplets (Chen and Wang, 2021). The *de novo* synthesis of TAG can also occur in the chloroplast (Fan et al., 2011). In *Chlamydomonas*, there are two families of diacylglycerol acyltransferase; type one contains DGAT1, and type two contains 5 different DGTT (Liu and Benning, 2013). DGAT1 and DGTT1 are shown to be upregulated under nutrient deprivation in *Chlamydomonas* (Boyle et al., 2012). TAG synthesis may not always be *de novo* in *C. reinhardtii* where a lipase called plastid galactoglycerolipid degradation 1 (PGD1) hydrolyzes the monogalactosyldiacylglycerol (MGDG) molecules into free fatty acids forming a carbon pool for TAG synthesis (Li et al., 2012).

In the final step, TAG molecules are packaged into a droplet-like structure known as lipid droplets (LD). LDs consist of a neutral lipid core and a phospholipid monolayer interrupted by the structural protein called major lipid droplet protein (MLDP) and enzymes involved in lipid biosynthesis, lipid trafficking, lipid catabolism, and vesicle trafficking (Goold et al., 2015). In *C. reinhardtii* cells, LDs are most commonly found distributed in the cytoplasm and more than 80% of those are found associated with the ER membrane. LD biogenesis initiates with oil lens formation (which occurs due to the coalescence of the oil phase) and LD budding from ER (Walther et al., 2017). When the TAG concentration is above the critical value, LD formation begins with the recruitment of proteins like SEIPIN and LD-associated protein (LDAP) (Li-Beisson et al., 2021). One of the main driving forces involved in LD biogenesis is liquid-liquid phase separation (LLPS). Due to a large equilibrium chemical potential, other TAG molecules spontaneously flow to the existing nascent LD molecule leading to LD expansion (Zoni et al., 2020). LDs vary greatly in size and number from one microalga species to another. For example, *C. reinhardtii* makes LDs of ~1.5µm while *Chlorella* sp. makes LDs of >3µm (Goold et al., 2015). The size and number of LDs depend on the environmental stress and the growth stage. The presence of MLDPs in the protein coat regulated the size of LDs (Li-Beisson et al., 2021).

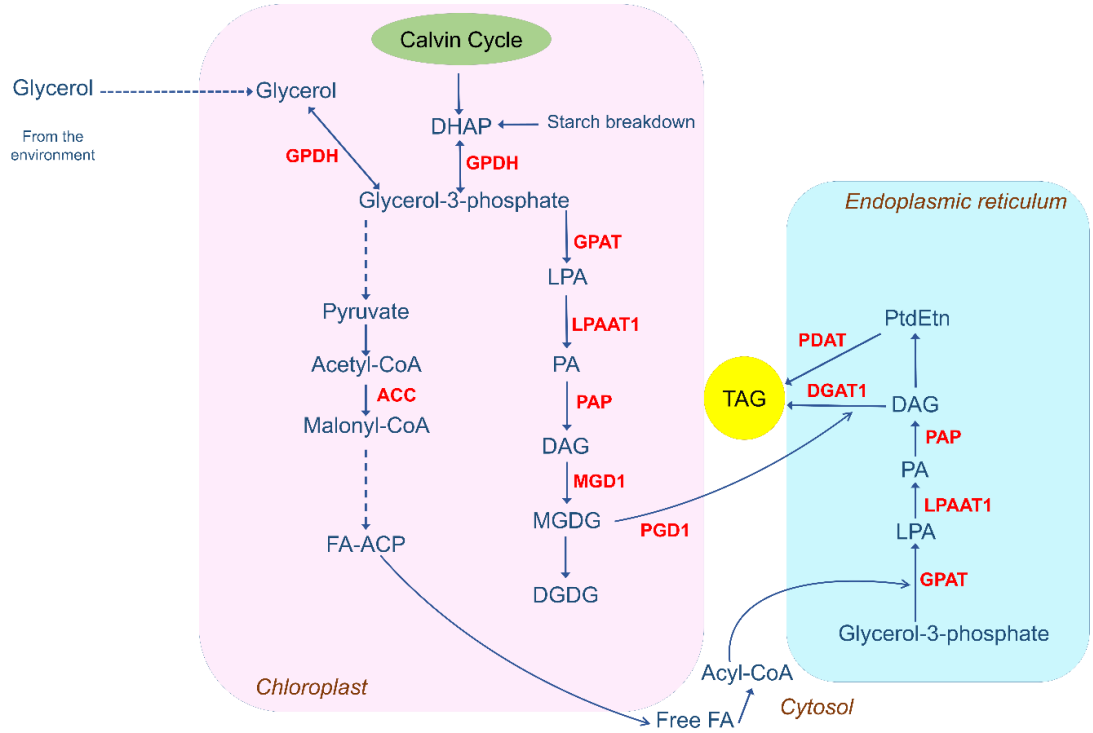

Figure 1.6. TAG biosynthesis pathway in microalgae.

Solid arrows represent single reaction steps and dashed arrows represent multiple reaction steps. **GPDH,** glycerol-3-phosphate dehydrogenase; **ACC**, acetyl-CoA carboxylase; **ACP**, acyl carrier protein; **DHAP**, dihydroxyacetone phosphate; **GPAT**, acyl-CoA:glycerol-3-phosphate acyltransferase; **LPA**, lysophosphatidic acid; **LPAAT**, acyl-CoA dependent acyl-CoA: LPA acyltransferase; **PA**, phosphatidic acid; **PAP**, phosphatidic acid phosphatase; **DAG**, diacylglycerol; **DGAT**, acyl-CoA: diacylglycerol acyltransferase; **TAG**, triacylglycerol; **MGDG**, mono galactosyl diacylglycerol; **DGDG**, di galactosyl diacylglycerol; **FA**, fatty acid; **PtdEtn**, phosphatidylethanolamine; **PDAT**, phospholipid: DAG acyltransferases.

1.4.2.2 Lipid catabolism and lipid droplet disassembly

Lipid droplet degradation initiates upon a specific environmental signal and is primarily executed by a DNA-binding protein called CHT7 (Compromised in TAG Hydrolysis 7). The first step is protein coat remodeling (**Figure 1.7**). When the optimum conditions are restored, LD hydrolysis is catered by MLDPs, and DTH1 (Delayed in TAG Hydrolysis 1). DTH1 contains a phosphatidylethanolamine (PtdEtn)-binding domain which induces a negative curvature in the LD membrane assisting in the membrane fusion and maintaining the LD integrity (Li-Beisson et al., 2021). PtdEtn is also responsible for activating the autophagy-related protein, ATG8. Disassociation of ATG8 with PtdEtn, due to a decrease in PtdEtn content in the LD membrane, results in ATG8 deactivation and hence lipid degradation (Lee et al., 2020). Once the protein coat is remodeled, TAG is broken down into free FA with the help of lipases and releases glycerol moiety in the process. LIP1 (a DAG lipase) and LIP4 (a TAG lipase) are responsible for TAG breakdown in *Chlamydomonas.* In addition to lipase-mediated lipid turnover, autophagy also plays a crucial role (Kong et al., 2018).

In the final step of lipid catabolism, fatty acid molecules are oxidized. FA oxidation can occur in both peroxisomes and mitochondria in microalgae. *Chlamydomonas reinhardtii* ensures physical contact between LDs and peroxisomes and FA breakdown by the β-oxidation pathway (Hayashi et al., 2015). Studies show that FAs are transported into peroxisomes by an ATP-binding cassette transporter (ABCD1) present in the peroxisomal membrane (Li-Beisson et al., 2015). Broken FAs can be used either for membrane lipid biosynthesis or to release carbon and energy for other cellular needs.

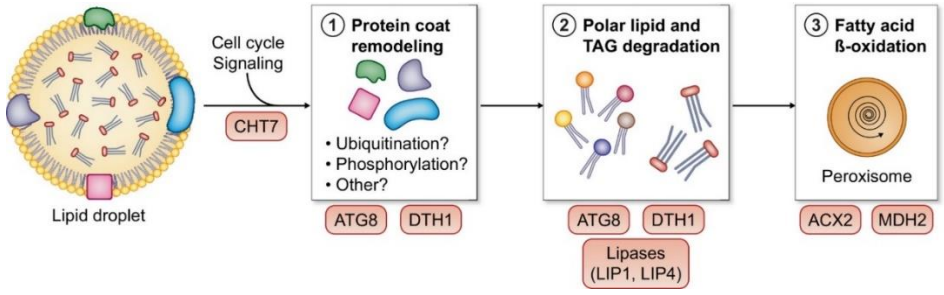

Figure 1.7. Lipid catabolism and lipid droplet degradation in *Chlamydomonas* sp.

CHT7, Compromised in TAG Hydrolysis 7; ATG8, autophagy-related protein 8; DTH1, Delayed in TAG Hydrolysis 1; LIP1 and LIP4, Lipase 1 and 4, respectively; ACX2, Acyl-CoA oxidase 2; MDH2, Malate Dehydrogenase 2 (Li-Beisson et al., 2021) (See Appendix A6.2. for copyright information).

1.4.3 Biosynthesis of photosynthetic pigments

Chlorophylls, carotenoids, and phycobilins are the main photosynthetic pigments in microalgae. The first two are fat-soluble while the last one is water-soluble.

Chlorophylls are the most abundant photosynthetic pigment in microalgae. There are five main types of chlorophylls (Chl); Chl *a*, *b*, *c*, *d*, and *f*. Their absorption maxima are 665 nm, 652 nm, 630 nm, 696 nm, and 707 nm, respectively. Chl *a* is the most abundant form and an essential component of the reaction center in photosystems. Chl *b* is an accessory pigment in green microalgae and the second most abundant pigment. Red algae contain Chl *d* while Chl *c* is widely distributed in Chromophytes and diatoms. Chl *f* has been recently reported in a few species of cyanobacteria (Carmo da Silva and Lombardi, 2020). The total amount of chlorophyll synthesized by a microalgal cell varies from 0.5-5% of dry cell weight as a function of the environmental condition and from one species to another (Harun et al., 2010). High light intensity reduces the chlorophyll content by 7 times in *Chlorella* sp (He et al., 2015). Low light intensity and nitrogen starvation, on the other hand, increase the chlorophyll content in *Scenedesmus dimorphus* (Ferreira et al., 2016). The change in a trophic condition also impacts chlorophyll production. Mixotrophy causes a reduction in the amount of chlorophyll in the exponential phase of *C. reinhardtii* but increases the production during the stationary phase (Puzanskiy et al., 2021).

Carotenoids are light-harvesting pigments that play an essential role in combating oxidative stress in microalgae (Pérez-Pérez et al., 2012). The type of carotenoid synthesized varies from one microalga to another. For example, *Dunaliella salina* contains majorly β-carotene, *Haematococcus pluvialis* produces astaxanthin, canthaxanthin, and lutein, *Chlorella vulgaris* synthesizes canthaxanthin and astaxanthin, *Scenedesmus almeriensis* accumulates lutein and β-carotene, *Chlamydomonas reinhardtii* produce β-carotene, violaxanthin, neoxanthin, lutein, and loroxanthin (Levasseur et al., 2020). The production of a specific type of carotenoid is also decided by environmental factors. For example, lutein productivity increases as the light intensity increases and decreases under nitrogen deprivation in *Chlorella zofingiensis* (Cordero et al., 2010). Astaxanthin is produced maximum at an optimum growth temperature of 28°C in *Haematococcus pluvialis* (Wan et al., 2014). High light intensity is also favorable for the production of β-carotene in *Dunaliella salina* (Ribeiro et al., 2011).

1.4.4 Role of carbon and nitrogen metabolism in regulating metabolite production

In photosynthetic algae, the metabolic flow of carbon and nitrogen interconnects carbohydrate, lipid, and protein metabolism (**Figure 1.8**).

1.4.4.1 The metabolic flow of carbon

TAG accumulation is mainly powered by either or all of these mechanisms: (1) *de novo* TAG synthesis; (2) recycling of C_2 moieties from degraded membrane lipids into TAG; (3) increased carbon flux towards glucose-3-phosphate and acyl-CoA for FA synthesis (carbon partitioning) (Jia et al., 2015).

The metabolic flow of carbon to lipid synthesis increases when microalgae are cultivated in heterotrophic or mixotrophic conditions. In a heterotrophic culture of *C. protothecoids*, compounds like starch, membrane lipids, proteins, and chlorophyll which are rich in carbon and nitrogen undergo degradation to release carbon and energy for lipid accumulation (Li et al., 2014). In nitrogen starvation, the carbon flux involved in nitrogen assimilation and protein metabolism is redirected to the formation of storage carbon compounds like starch and TAG. Starch and TAG are two important and competing energy sinks in algal and plant cells (Tan et al., 2016). As shown in *C. reinhardtii*, the carbon source is a key metabolic factor regulating carbon partitioning between starch and lipids (Fan et al., 2012).

The carbon partitioning phenomenon is highly subjective to the nutrient availability in the environment and varies among different microalgae. For example, *Dunaliella tertiolecta* prefers to make starch as the storage compound because it is energetically cheaper than TAG synthesis. *C. reinhardtii* and *Chlorella vulgaris* accumulate energy-intensive TAG molecules (Tan et al., 2016). One of the key enzymes responsible for the starch-to-lipid switch is triose phosphate isomerase (TPI). High levels of TPI activity result in increased conversion of G3P to DHAP, finally leading to starch synthesis, and low levels of TPI activity cause increased accumulation of G3P which is fluxed into acetyl-CoA production and hence FA biosynthesis (Chang et al., 2016). Starch degradation is achieved by amylases (α, β, and iso) and starch phosphorylase (SP) (Ran et al., 2019). Manipulation of environmental factors like an increase in salinity has been observed to induce starch-to-lipid switch by activating SP and

amylases resulting in excessive TAG accumulation in *C. reinhardtii* (Ho et al., 2014b). Similarly, excessive phosphorous in nitrogen-depleting conditions diverts the switch to lipid production by activating AGPase activity in *Chlorella* sp. (Nayak et al., 2019).

1.4.4.2 The metabolic flow of nitrogen

Carbon and nitrogen metabolism are very closely interlinked inside the microalgal cell. When microalgal cells are exposed to abiotic stress conditions, like nitrogen deprivation, *de novo* protein synthesis is inhibited and protein degradation and turnover begin to release free amino acids inside the cell which are later converted to lipids (**Figure 1.8**) (Hildebrandt et al., 2015). The three important junction points of the C/N cycle are guarded by enzymes pyruvate kinase (PK), citrate synthase (CS), and glutamate decarboxylase (GAD), which catalyzes pyruvate metabolism, TCA cycle, and amino acid metabolism, respectively (Chen and Wang, 2021) (**Figure 1.8**).

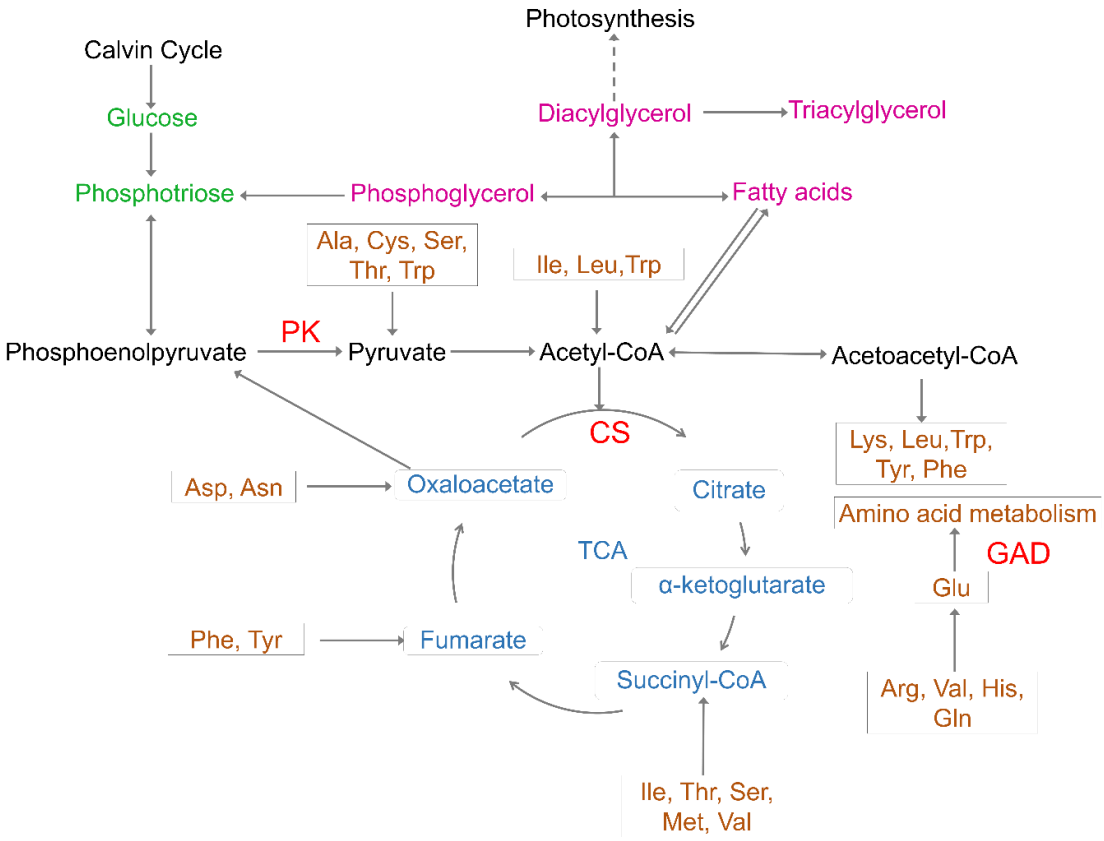

Figure 1.8. Interconnection between metabolic pathways of photosynthesis, lipid synthesis, protein metabolism, and starch metabolism in microalgae.

The ones highlighted in green color font represent the carbohydrate metabolism products, purple represents lipid metabolism, brown represents protein metabolism, blue represents the TCA cycle and black are the intermediates. CS, citrate synthase; GAD, glutamate decarboxylase; PK, pyruvate kinase; TCA, tricarboxylic acid.

1.4.5 Role of signaling pathways in lipid metabolism

Under abiotic stress conditions, different signaling pathways are known to regulate lipid metabolism which is summarized below.

1.4.5.1 Ca^{2+} signaling pathway

Ca^{2+} is a ubiquitous signal transduction messenger molecule that plays an important role in relaying the changes in environmental conditions like changes in CO_2, O_2, light, nutrient concentration, or any other stress (Chen and Wang, 2021). The membrane-bound and intracellular Ca^{2+} sensor proteins in *Chlorella* sp. are known to regulate lipid biosynthesis under nitrogen deprivation (Chen et al., 2015).

1.4.5.2 MAPK-signaling pathway

The key players of the MAPK (mitogen-activated protein kinase) pathway are JNK (c-Jun N-terminal kinase), ERK (extracellular signal-regulated kinase), and p38 MAP kinase (Chen and Wang, 2021). cAMP (cyclic adenosine monophosphate) is also related to lipid production regulation in *C. reinhardtii* and *C. vulgaris* (Choi et al., 2015). JNK and ERK, both are known to upregulate lipid biosynthesis under salinity stress in *Chlamydomonas reinhardtii* (Yang et al., 2018).

1.4.5.3 ROS signaling pathway and autophagy

Reactive oxygen species (ROS) like superoxide anion, singlet oxygen, hydrogen peroxide, and hydroxyl radical act as second messengers in the signal transduction pathway, inducing lipid accumulation in microalgae (Chen and Wang, 2021). ROS molecules link the effect of abiotic stress, lipid accumulation, and the process of autophagy (Perez-Perez et al., 2012) (**Figure 1.9**).

Autophagy initiates the formation of a double-membrane vesicle called autophagosome which then fuses with the lysosome for degradation and turnover of ROS-mediated oxidized components of the cell. Autophagosome is formed by autophagy-related proteins called ATG. ATG5, ATG12, and ATG16 together form a complex and mediate the formation of the autophagosome along with ATG8-PtdEtn (**Figure 1.10**). Here, ATG8-PtdEtn is important for the fusion of the autophagosome with the lysosome.

ATG4 is a cysteine protease that activates ATG8. Another protein called ATG1 is a kinase that is responsible for autophagy initiation. ATG1 is further regulated by the TOR (Target Of Rapamycin) kinase, which is an autophagy inhibitor (Perez-Perez et al., 2012; Pérez-Pérez et al., 2017b).

TOR kinase forms a multiprotein complex called TOR complex 1 and 2 (TORC1 and TORC2). TORC1 proteins, LST8 and KOG1/Raptor, play an essential role in regulating autophagy in *Chlamydomonas*. TORC1 phosphorylates ATG13, a subunit of ATG1, thereby deactivating it and inhibiting autophagy. TORC1 forms the target of rapamycin. Other than lipid biosynthesis, TORC1 is also known to control protein synthesis in *Chlamydomonas* (Pérez-Pérez et al., 2017a). TOR signaling is involved in lipid accumulation under nutrient deprivation, but the molecular details of the mechanism remain to be identified. Carotenoid depletion also triggers ROS-induced lipid accumulation in *C. reinhardtii* (Pérez-Pérez et al., 2012).

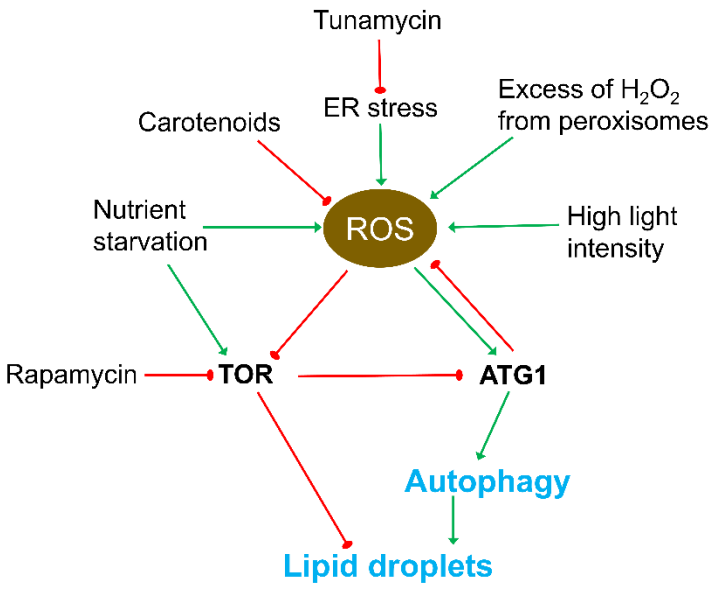

Figure 1.9. ROS-mediated regulation of autophagy and lipid production in microalgae.

Red-colored blunt-end arrows indicate inhibition and green-colored arrows indicate activation of the molecule.

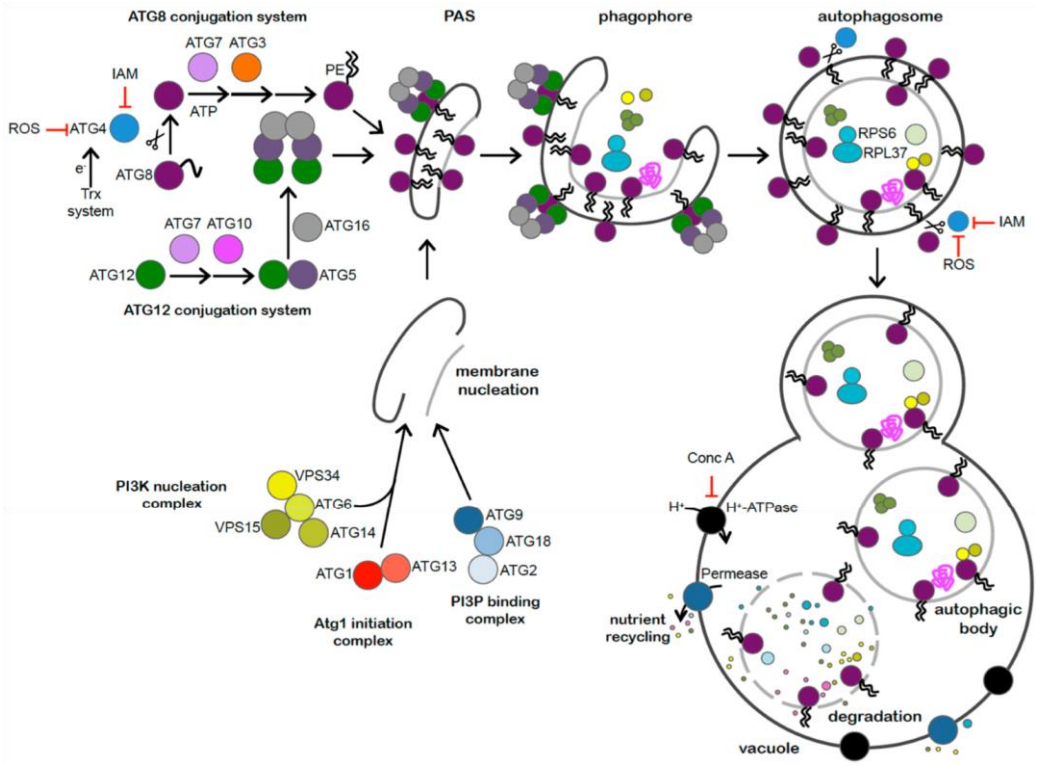

Figure 1.10. Autophagosome formation in *Chlamydomonas*

Adapted from (Pérez-Pérez et al., 2017a) (See Appendix A6.3. for copyright information).

1.5 Techniques used to study the production of starch, chlorophyll, carotenoids, and lipids

Various techniques are used to detect metabolite concentration and composition in microalgae. The biochemical assays have been replaced by modern ways of estimations which include biophysical, bioinformatics, and computational methods (**Table 1.3**). The most conventional methods being used worldwide are spectrometric, integrated with GC, TLC, LC, or HPLC, and spectrophotometric methods (UV-VIS). The new-age techniques are NMR, FTIR/NIR, and Raman spectroscopy. Imaging methods like staining lipids with Nile red dye/BODIPY, starch with iodine, and direct imaging of pigments, micro-Raman spectroscopy have also become popular given the minimum processing steps and high-resolution observations. With recent advances, microfluidic systems have also paved the way to study metabolite production in microalgae.

1.5.1 UV-VIS Spectrophotometry

Using a UV-VIS spectrophotometer, cell density and photosynthetic pigments like chlorophylls and carotenoids can be easily quantified. Microalgal cell density can be measured at 680 nm or 750 nm. The pigments, being hydrophobic can be extracted in organic solvents like ethanol, isopropanol, methanol, and acetone and are estimated at their characteristic absorption maxima. Carotenoids are estimated at 470 nm of the electromagnetic spectrum (Lichtenthaler et al., 2005). The starch content of microalgal cells can also be quantified by extracting starch in Lugol's solution and estimating the blue-colored starch-Lugol complex using a spectrophotometer (Black et al., 2013). With time, assays have been developed to quantify free fatty acid content and even the biodiesel content in the biodiesel/diesel blend (Azeman et al., 2015; Silva et al., 2015). The UV-VIS spectrophotometer is a rapid, handy, and affordable technique to run preliminary estimations. However, the preparation of the sample for spectrophotometric estimation is a complex, multi-step, and laborious procedure. Moreover, the estimates are an average result of only a fraction of the sample.

Table 1.3. Conventional biochemical methods *versus* new-age biophysical techniques used for the analysis of biomolecules in microalgae

Conventional methods	Metabolite detected	Advantages/ Disadvantages	Advanced biophysical methods	Advantages/ Disadvantages	References
Gas /Liquid chromatography coupled with a Mass spectrometer (GC-MS / LC-MS)	Fatty acids, carbohydrates, proteins	Advantages: high sensitivity, applicable to a broad range of thermally labile samples, detects the fatty acid composition and biofuel quality Disadvantages: restricted to low volatility samples, requires large culture volume, polar metabolites need prior derivatization, lipids need to be extracted from biomass, calibration lipids needed	Raman spectroscopy (micro-RS, LTRS, SCRS, CARS, SERS, Resonance RS)	Advantages: non-invasive, *in vivo* detection, applicable to small volume cultures, simultaneous multivariate analysis, detect the fatty acid composition and biofuel quality Disadvantages: background fluorescence in microalgae, photodamage due to high-energy lasers	(Breuer et al., 2013; Calixto et al., 2018; Guidetti Vendruscolo et al., 2019; Paul et al., 2019; Huang et al., 2010; Hounslow et al., 2017; Nekvapil et al., 2022)
High-performance liquid chromatography (HPLC)	Carbohydrates triacylglycerol fatty acids, amino acids, carotenoids	Advantages: identifies free fatty acids and carotenoids, rapid, high sensitivity Disadvantages: extensive sample preparation steps, labor-intensive procedure	Fourier transform infrared spectroscopy (FTIR)	Advantages: rapid, whole cell analysis, non-destructive, small volume sampling, simultaneous determination Disadvantages: the presence of water affects the spectral readings and extensive sample preparation steps	(Liu et al., 2020; Osterrothová et al., 2019; Patras et al., 2018; NGUYEN et al., 2017)
UV-Visible spectrophotometry	Proteins, carbohydrates, chlorophyll, carotenoids	Advantages: simple to interpret quantification of metabolites, affordable and handy technique	Nuclear magnetic resonance (NMR) – solid-state and liquid-state, 2D-NMR	Advantages: non-invasive, accurate, structural quantitative determination, independent of the size of the metabolite,	(Bisht et al., 2021; Lichtenthaler et al., 2005; Arnold

		Disadvantages: difficult derivatization of the metabolite, multiple sample processing steps, interference from unwanted absorbents present in the solution		whole-cell quantification, no sample extraction required Disadvantages: expensive, spectrum analysis is difficult and time-consuming.	et al., 2020; Warnet et al., 2015; Silva et al., 2015)
Conventional fluorescence imaging and spectroscopy	Lipids, starch, chlorophyll	Advantages: in-cell detection, imaging enables cellular localization detection, direct quantification of chlorophylls, detect cellular level changes, real-time monitoring Disadvantages: lipid and starch quantification require labeling, reactive oxygen species quench fluorescence, might need sample dilution	Fluorescence hyperspectral imaging, fluorescence lifetime microscopy, fluorescence polarization anisotropy microscopy, fluorescence recovery after photobleaching	Advantages: simultaneous multi-organelle imaging and real-time dynamics, lipid/pigment composition as well as quantity, micro-scale mechanical properties, and molecular organization in cells. Disadvantages: requires fluorescent labeling, advanced instrumentation, and detectors.	(Wunder et al., 2018; Davis et al., 2014; Lian et al., 2021; Karpf et al., 2017; Guan et al., 2022)
Atomic force microscopy	Application of compressive stresses, the study of microalgae under mechanical stress	Advantages: nano-scale resolution, molecular interactions can be studied, no labeling required, allows nanomechanical measurements, interactions of the cell with the environment, cell wall rigidity can be studied Disadvantages: expensive, slow scanning speed	Droplet microfluidics	Advantages: application for high throughput optimization, efficient single cell sorting, and imaging, application of various types of mechanical forces such as shear, compressive, oscillatory, and laminar flow. Disadvantages: fabrication of microfluidic chambers, optimizations needed for channel size and shape, and good control of fluid flow.	(Liu et al., 2020; Demir-Yilmaz et al., 2021; Warren et al., 2014; Kim et al., 2017, 2018; Sart et al., 2022)

1.5.2 Fluorescence spectroscopy

Fluorescence is defined as the phenomenon where an excited singlet state of the electron comes back to the ground state emitting photons with higher wavelength and reduced energy compared to the incident photons. However, lipid molecules lack inherent fluorescence properties and their detection needs labeling with a fluorophore before determination. Intrinsic fluorophores include NAD(P)H, chlorophyll, aromatic amino acids, vitamins, and cofactors. Some major concerns while working with fluorescent molecules are, 1) an optimally dense solution for accurate fluorescence capture, 2) to avoid substances like free radical oxygen species that can aid in quenching the fluorescence, and 3) to eliminate photobleaching due to high-intensity laser that can irreversibly transfer the fluorophores to a permanent dark state. Also, many extrinsically labeled fluorophores have a short half-life and extinction coefficient and degrade with time (Sá et al., 2022; Liu and Christopher Q. Lan, 2014).

Chlorophyll fluorescence in microalgae can be measured at red-far red wavelengths falling in the range of 650-850 nm. It is an effective method to determine the photosynthetic efficiency of microalgal cells which changes under abiotic stress or with aging (Liu et al., 2020). For example, chlorophyll fluorescence has been used to study the photosynthetic efficiency under phosphorous stress in *C. vulgaris* (Jiao et al., 2017). Pulse Amplitude Modulated (PAM) fluorometry is often used to measure the fluorescence kinetics of chlorophyll. Such an analysis in red algae has shown reduced activity of the PSII reaction center in nitrogen deficiency (Zhao et al., 2017). The use of NAD(P)H fluorescence enables measuring the biomass and the metabolic state of the microalgal cells. It is excited at 340 nm wavelength and emits fluorescence at 460 nm (Sá et al., 2022).

For lipids, commonly used lipophilic fluorescent dyes are Nile Red and BODIPY. The excitation-emission wavelengths vary for neutral lipids (shorter emission wavelength, <590 nm) and total lipids (>590 nm) which also include polar lipids. Nile red has an excitation wavelength of 488-525 nm and an emission of 570-600 nm. The most commonly preferred solvents compatible with this range are DMSO, EDTA, and glycerol. The NR uptake by the cell is also affected by the cell wall in microalgae. The temperatures of 30- 40 ℃ can effectively cause diffusion through thick cell walls. The interaction between NR dye and lipids can be further improved by using a low dye: cell density ratio (Liu and Christopher Q. Lan, 2014; Hounslow et al., 2017; Patel et al.,

2019). Fluorescence spectrometry is a high-throughput method to successfully reveal the cellular lipid content (Lee et al., 2013b). Since NR measurement is relative, triolein is often used as a standard to obtain absolute quantification (Bertozzini et al., 2011). BODIPY is an alternate method of studying lipid concentration. It is more photostable than NR and its fluorescence spectrum does not overlap with that of chlorophyll. It has a high quantum yield, narrow emission spectrum (505-515 nm), higher sensitivity, and better reproducibility. It can be dissolved easily in DMSO at concentrations 100 times lesser than NR. However, pretreatment of the sample to allow full permeation of dye molecules might hinder cell growth and can result in an ineffective method (Hounslow et al., 2017; Patel et al., 2019).

1.5.3 Raman spectroscopy (RS)

RS is based on the principle of Raman scattering. When an incident monochromatic light strikes the sample molecules, the light scattered with different frequencies forms Raman scattered light. The incident beam of light polarizes the vibrational state of the molecule resulting in an energy shift (represented as wavenumber, cm^{-1}), that is specific to the vibrational modes and rotational modes of the analyte molecule. As a result, each chemical bond produces a characteristic Raman spectrum, called a fingerprint. However, there is always a strong Rayleigh scattering in the sample (scattering at the same frequency) which interferes with the Raman signal at small wavenumbers and has to be eliminated by a suitable Notch filter (Liu et al., 2020; Hounslow et al., 2017).

Raman spectroscopy can be used for both qualitative and quantitative analysis. The height of the Raman peak formed in the spectrum represents the amount of the functional group. However, absolute quantification requires calibration with a known standard. RS has been extensively used to study the composition and concentration of lipids, starch, chlorophyll, carotenoids, and proteins in microalgae grown under different environmental conditions (Liu et al., 2020; Hounslow et al., 2017). Rapid in-vivo quantification of lipids and carotenoids could be achieved using RS in *Chlorella vulgaris* (Lee et al., 2013c). RS is also capable of differentiating between C-C single bond and a double bond, thereby evaluating the degree of unsaturation of the fatty acid molecules along with their chain length (Sharma et al., 2015). RS is a non-invasive and rapid tool to identify different types of biomolecules present in the microalgal sample

in a single screening. The ability of RS to quantify lipids has also been validated by GC-MS (He et al., 2017b).

Raman scattered signals can be collected by an objective in a confocal geometry, called micro-Raman spectroscopy or single-cell Raman spectroscopy (SCRS). SCRS has been used to simultaneously quantify lipids, starch, and proteins in *C. reinhardtii* along with deduction of unsaturation degree with an accuracy of ~99%, in nitrogen-replete and nitrogen-deplete conditions (He et al., 2017b). SCRS has also been used in microalgal species like *Haematococcus pluvialis,* where it was used to identify the type of carotenoid synthesized in presence of excess CO_2 (Patel et al., 2019). Recently, with the help of SCRS, "ramanome" was generated for 27 phylogenetically diverse microalgal species, and some unidentified cells were functionally characterized and identified with the help of Raman-activated sorting and sequencing (Baladehi et al., 2021).

Several modifications to the traditional Raman spectroscopy have been made to enhance the signal-to-noise ratio of the Raman signal. For example, single cell-LTRS (optical tweezers Raman) has been used extensively to study microalgal lipids produced by N-depleted microalgal culture (Wu et al., 2011). The coherent anti-stokes Raman (CARS) microscopy was applied to study the unsaturation content of the fatty acid molecules produced by oleaginous microalga *Monoraphidium neglectum* (Jaeger et al., 2016). CRS, confocal Raman spectroscopy, was used for the qualitative estimation of lipids and carotenoids in *C. sorokiniana* (Huang et al., 2010). With the help of surface-enhanced Raman spectroscopy (SERS), quantitative estimation of carotenoid, fucoxanthin was performed in a diatom, revealing several important aspects of diatom growth (Nekvapil et al., 2022). The high resolution obtained in SERS is capable of distinguishing the carotenoid and lipid Raman peak in single microalgal cells grown under stress and invariably dictates the unsaturation content in their lipids (Ramya et al., 2017).

Although advancements have manifested an accurate determination of metabolites in microalgae, some limitations of the technique cannot be overlooked. While working with photosynthetic organisms, it is important to negate the background fluorescence of photosynthetic pigments (Huang et al., 2010). For example, the Raman peak of β-carotene can interfere with the lipid band. The other limitation in the case of microalgae

is the use of the monochromatic laser of 532 nm with high energy to obtain clear Raman peaks. However, it may cause photo-damage to the cells. In such a case, a laser of 785 nm can be used but with a compromised scattering (Hounslow et al., 2017).

1.5.4 Microscopy

Microscopy is a high-resolution, non-invasive, and rapid technique for biomolecular identification in space and time. With a high-end confocal microscopic approach, it is possible to study beyond the dominant behavior, size, and sub-cellular localization of lipid droplets in microalgal cells. Time-course experiments can illustrate how these properties change with advancing age and under the effect of abiotic stress. Live-cell microscopic observation of LDs post-Nile red staining is a popular age-old method being used since 1985 (Greenspan et al., 1985) and never fails to deliver quick subcellular localization and quantification of LDs in stressed microalgal cells (Rugnini et al., 2020). Recently, Oil red O (ORO) has emerged as a cheap and non-toxic replacement for Nile red to stain LDs in microalgae (Marquez and Beccaria, 2020). High-end microscopy like transmission electron microscopy (TEM) has made possible the determination of lipid droplet size and their interactions with other cellular structures, like autophagosomes (Tran et al., 2019b; Tarazona Delgado et al., 2021). Atomic force microscopy helped to understand that the cell size and cell wall thickness increase in the nitrogen-deprived cells of *Chlorella* sp. (Yap et al., 2016). The other popular fluorescence imaging method is chlorophyll auto-fluorescence. Using Chl fluorescence imaging, the single-cell photosynthetic activity could be determined in microalgae (Trampe et al., 2011). In an advanced system based on the combination of optics and microfluidics, the combination of fluorescence, Raman spectroscopy, and microscopically-abled flow cytometry allows the determination of live cells, lipid production, and the heterogeneity present in the microalgal cells (Zheng et al., 2021). Microscopic-based single-cell study of lipid droplets and chlorophyll distribution is also validated by fluorescence measurements from a spectrometer (Sandmann et al., 2018).

1.6 Single-cell analysis in microalgal biofuel production

Cell-to-cell differences always occur in a population and give rise to phenotypic heterogeneity in cell growth, stress resistance, and metabolite production, even in an isogenic population (Wang et al., 2014b). These variations in the cell phenotype are crucial for the cells to adapt to stressful conditions. There is always a subpopulation of cells that deviate from the total population to undergo adaptation. This subpopulation can be captured only if studied at a single-cell level and over time (Lidstrom and Konopka, 2010; Martins and Locke, 2015). The average phenotype obtained from bulk assays fails to answer the hidden variations in the population characteristics (Altschuler and Wu, 2010). Population distribution analysis can be performed using high-resolution techniques like micro-Raman spectroscopy or confocal microscopy to study lipid distribution and heterogeneities in the population (Lee et al., 2013a; He et al., 2017b; Wang et al., 2014c). It is imperative to understand how population-level study overlooks the single-cell level changes which are important to understand the effect of any stress on a population (**Figure 1.11**).

Single-cell microscopy studies the lipid droplet size, density, distribution, chloroplast, and chlorophyll degradation as an effect of N-starvation and reveals heterogeneity in *Acutodesmus obliquus* (Sandmann et al., 2018). Microfluidics-based high throughput screening also dictates the heterogeneity in the lipid production produced by the microalgal cells of the same culture under nitrogen starvation conditions (Zheng et al., 2022). With the help of a specialized device called “PhenoChip”, Behrendt and the group carried out single-cell monitoring of microalgae for their photosynthetic efficiency and thermal tolerance (Behrendt et al., 2020). This chip is expected to deliver useful information on strain selection for efficient biofuel production. Single-cell metabolomics using high-resolution mass spectrometry determines cellular physiology and enables the characterization of the population into different groups based on their stress tolerance (Baumeister et al., 2019). High-resolution based Raman flow cytometry was used to quantify the starch and screen cells for higher content produced under environmental anomalies with sensitivity higher than the commonly used Lugol’s iodine method (Gala de Pablo et al., 2023). These methods described here are not only non-invasive and label-free but also labor-intensive for efficient high-throughput

screening procedures. These simultaneously uncover the heterogeneities associated with metabolite production, especially under abiotic stress.

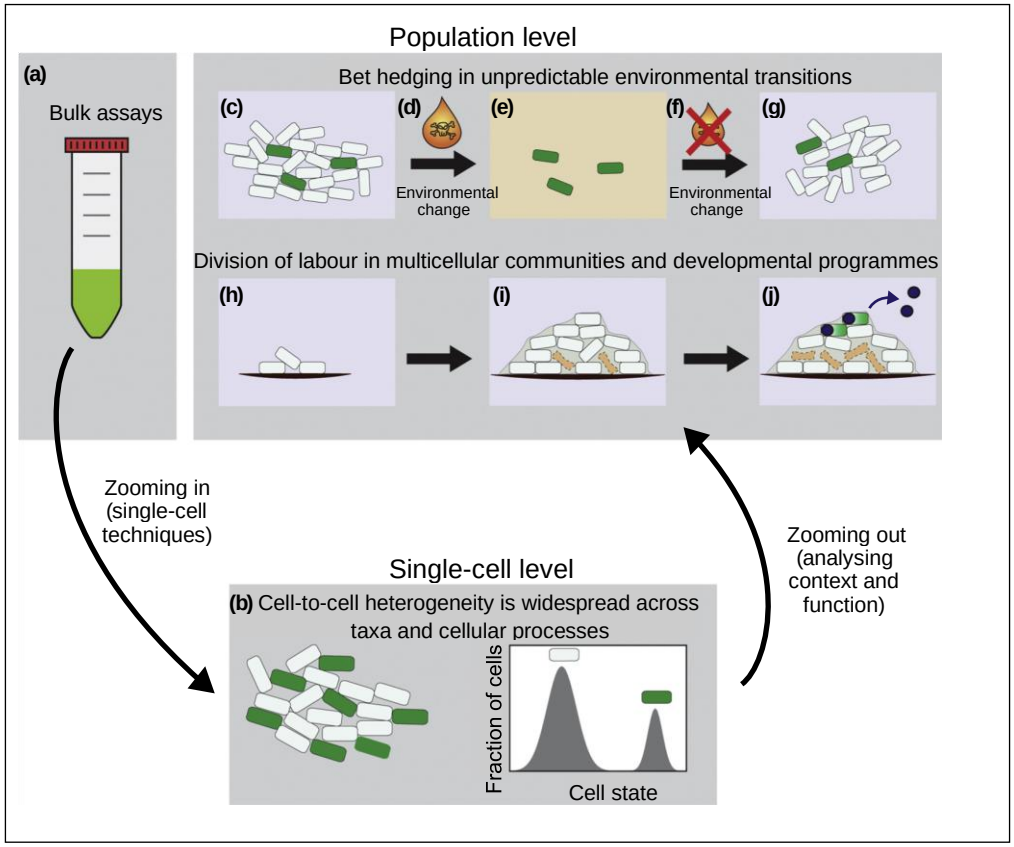

Figure 1.11. The loop between population-level and single-cell-level studies.

Adapted from (Martins and Locke, 2015) (See Appendix A6.4. for copyright information)

1.7 The model microalga- *Chlamydomonas*

Chlamydomonas is a motile unicellular green microalga with about 150 species. It is oval-shaped and generally grows in freshwater, although some species are also found in marine water and even in snow. It can be efficiently grown in both open ponds and closed photo-bioreactors with flat plates, and tubular or vertical columns with controlled CO_2 flow (Missoum, 2019). A representative structural diagram of *Chlamydomonas reinhardtii* is shown in **Figure 1.12**. The whole genome of *C. reinhardtii* was sequenced in the year 2007 (Merchant et al., 2007). The proteomics and transcriptomics approach in *Chlamydomonas* has made it easier to understand the metabolic pathways responsible for bioenergy feedstock production and improve the productivity for large-scale production (Aucoin et al., 2016). It serves as a model organism for the application of a systems biology approach for efficient biofuel generation (Rupprecht, 2009). It has also been established as an industrial biotechnological host for metabolic engineering (Scaife et al., 2015). Using these advanced approaches, the database for enzyme kinetics involved in biofuel production has been generated to help in metabolic engineering in *C. reinhardtii* (Arend et al., 2022). This makes the organism an ideal model for the fourth generation biofuel source. Past few years, CRISPR-based technologies have become popularly used in this model alga to enhance the productivity of valuable bio-products (Lee et al., 2023).

Chlamydomonas is also a model microalga to study the role of autophagy in lipid production under stress and has led to the development of several autophagy monitoring methods in microalgae (Pérez-Pérez et al., 2017a). The study so far has revealed many essential aspects of the TOR-signaling network, the role of carotenoids in autophagy, ER stress, oxidative stress, and autophagosome formation in lipid production (Davey et al., 2014; Couso and Crespo, 2017; Couso et al., 2017; Perez-Martin et al., 2014; Tran et al., 2019b). Recently, it has been tested with biodegradable nanoparticles to increase lipid production via ROS-induced autophagic pathways (Lu et al., 2023). The study of *Chlamydomonas* has unveiled critical information about lipid metabolism and accumulation in the form of droplets, droplet assembly, and disassembly (Kong et al., 2018; Li-Beisson et al., 2021, 2015). Detailed profiling in *C. reinhardtii* has revealed the production of monounsaturated and polyunsaturated fatty acids (most desirable for good biodiesel quality) under nutrient deprivation and mixotrophy (James et al., 2011; Moon et al., 2013). It has also been extensively studied to produce biofuel by

simultaneously sequestering carbon dioxide from the environment (Banerjee et al., 2021). Several features of salt stress, like the key metabolic enzymes, the pathways involved, and the biomarkers of salt stress have been well-characterized in *C. reinhardtii* with implications in future biofuel research under such stress conditions in other microalgae (Bazzani et al., 2021). The novel mechanism of step-wise addition of salt was first conducted on *Chlamydomonas* sp. JSC4 and has been shown to produce improved biomass and lipid content (Ho et al., 2014b). In another independent study, the unique approach of fed-batch mixotrophic cultivation of *C. reinhardtii* has shown increments in biomass density and productivity (Fields et al., 2018). The simplicity of the *Chlamydomonas* genome and its cultivation has led to several important research in the area of biofuel production (Missoum, 2019). These aspects of *Chlamydomonas* research makes this organism an ideal model for innovative studies and establish research findings for future improvements in biofuel industry.

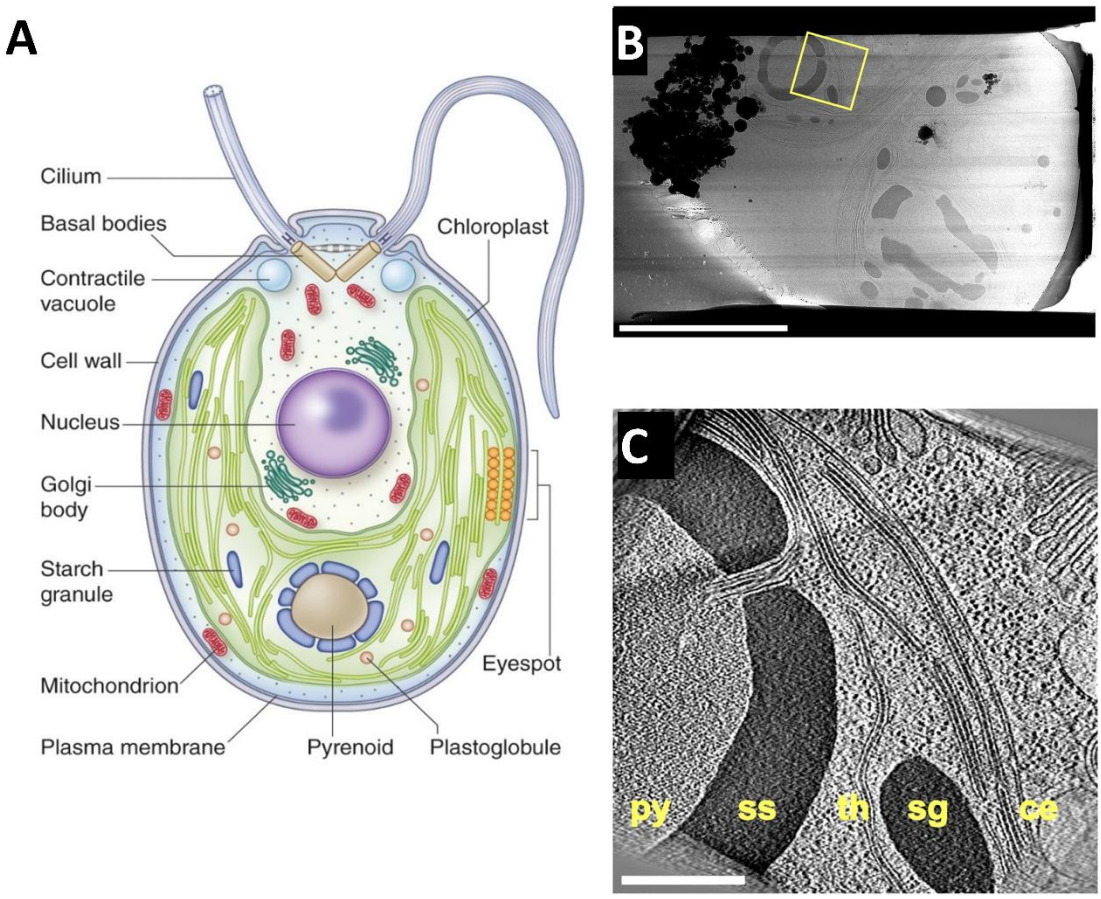

Figure 1.12. Diagrammatic representation of the structure of *Chlamydomonas reinhardtii* and the Cryo-EM FIB of frozen cells.

A.The cross-sectional representation of the *Chlamydomonas* cell shows all the organelles, with green-colored chloroplast occupying the maximum space of the cell. **B**. TEM high-defocus montaged overview of the chloroplast lamella. Scale bar in 5 µm. **C.** The tomographic volume represents the yellow box in **B**. Here, py is the pyrenoids surrounded by an "ss", starch sheath and "th", thylakoids, "sg", starch granule, and the "ce", chloroplast envelope. Golgi stacks and rough endoplasmic reticulum can be spotted at the upper right corner, along with both cytoplasmic and chloroplast ribosomes. The tomogram was 2× binned. Unbinned pixel size: 9.6 Å. Scale bar in 500 nm (Sasso et al., 2018; Engel et al., 2015)**.**

1.8 The foundation of the study

Among the several challenges faced in the current research on algal biofuel production, the top-priority challenge is to conserve the microalgal biomass under biofuel-inducing abiotic stress conditions and increase biofuel productivity. Scaling up the production from the bench to pond cultivation, oil extraction, and downstream processing are some other important challenges faced at the large-scale production level. To address the challenges, this study adopts two main strategies: 1) study the effect of modifications in the cultivation method on biomass and metabolite production, and 2) characterize the heterogeneous production of these metabolites at the single-cell level responsible for low yields of biomass under the given cultivation strategy.

Chlamydomonas reinhardtii CC-125 is used as a model to study the effect of two different abiotic stress conditions, salt stress, and carbon availability. As a part of the first strategy, single-stage, two-stage, and stepwise addition of stress factors are employed and their impact on cell density, starch, lipids, chlorophyll, and carotenoids is studied at the bulk level. It would be interesting to note if there is any preferential production of metabolites varying as the function of the cultivation strategy.

Single-cell level studies are performed to address the underlying population-scale heterogeneity in the metabolite production that exists in a single culture. Micro-Raman spectroscopy and fluorescence microscopy are used as tools for high-resolution studies. Using fluorescence microscopy, the impact of stress conditions on the cell size and shape, lipid droplet size and distribution, and their subcellular localization are studied. The possible mechanism involved in governing the size of the lipid droplets as a function of time and stress is further explored. Micro-RS is used as a high-throughput and rapid tool to uncover the metabolite details of the cell. It cuts down the tedious and cumbersome procedures involved in biochemical analytical methods. It is optimized to reveal details of lipid properties and pigment identification under stress.

Thus, working with these strategies altogether aims to minimize the ambiguity in biofuel production which would directly affect biofuel productivity at the industrial scale and also increase the cost-effectiveness of the process in the future.

1.9 References

Abdel-Raouf, N., A.A. Al-Homaidan, and I.B.M. Ibraheem. 2012. Microalgae and wastewater treatment. *Saudi J. Biol. Sci.* 19:257–275. doi:10.1016/j.sjbs.2012.04.005.

Abomohra, A.E.F., A.H. El-Naggar, S.O. Alaswad, M. Elsayed, M. Li, and W. Li. 2020. Enhancement of biodiesel yield from a halophilic green microalga isolated under extreme hypersaline conditions through stepwise salinity adaptation strategy. *Bioresour. Technol.* 310:123462. doi:10.1016/j.biortech.2020.123462.

Alalwan, H.A., A.H. Alminshid, and H.A.S. Aljaafari. 2019. Promising evolution of biofuel generations. Subject review. *Renew. Energy Focus*. 28:127–139. doi:10.1016/j.ref.2018.12.006.

Ali, H.E.A., E.A. El-fayoumy, W.E. Rasmy, R.M. Soliman, and M.A. Abdullah. 2021. Two-stage cultivation of *Chlorella vulgaris* using light and salt stress conditions for simultaneous production of lipid, carotenoids, and antioxidants. *J. Appl. Phycol.* 33:227–239. doi:10.1007/s10811-020-02308-9.

Altschuler, S.J., and L.F. Wu. 2010. Cellular Heterogeneity: Do Differences Make a Difference? *Cell*. 141:559–563. doi:10.1016/j.cell.2010.04.033.

Arend, M., D. Zimmer, R. Xu, F. Sommer, T. Mühlhaus, and Z. Nikoloski. 2022. Proteomics and constraint-based modelling reveal enzyme kinetic properties of *Chlamydomonas reinhardtii* on a genome scale. *bioRxiv*. 2022.11.06.515318.

Arnold, A., J. Bourgouin, B. Genard, E. Dror, R. Tremblay, I. Marcotte, A. Arnold, J. Bourgouin, B. Genard, D.E. Warschawski, and R. Trem-. 2020. Whole cell solid-state NMR study of *Chlamydomonas reinhardtii* microalgae To cite this version : HAL Id : hal-02567652 Whole cell solid-state NMR study of *Chlamydomonas reinhardtii* microalgae .

Atikij, T., Y. Syaputri, H. Iwahashi, T. Praneenararat, S. Sirisattha, H. Kageyama, and R. Waditee-Sirisattha. 2019. Enhanced lipid production and molecular dynamics under salinity stress in green microalga *Chlamydomonas reinhardtii* (137C). *Mar. Drugs*. 17. doi:10.3390/md17080484.

Aucoin, H.R., J. Gardner, and N.R. Boyle. 2016. Omics in *Chlamydomonas* for biofuel production. *In* Lipids in Plant and Algae Development, Subcellular Biochemistry. 447–469.

Azeman, N.H., N.A. Yusof, J. Abdullah, R. Yunus, M.N. Hamidon, and R. Hajian. 2015. Study on the spectrophotometric detection of free fatty acids in palm oil utilizing enzymatic reactions. *Molecules*. 20:12328–12340. doi:10.3390/molecules200712328.

Aziz, M.M.A., K.A. Kassim, Z. Shokravi, F.M. Jakarni, H.Y. Lieu, N. Zaini, L.S. Tan, S. Islam, and H. Shokravi. 2020. Two-stage cultivation strategy for simultaneous increases in growth rate and lipid content of microalgae: A review. *Renew. Sustain. Energy Rev.* 119:109621. doi:10.1016/j.rser.2019.109621.

Baek, K., J. Yu, J. Jeong, S.J. Sim, S. Bae, and E.S. Jin. 2018. Photoautotrophic production of macular pigment in a *Chlamydomonas reinhardtii* strain generated by using DNA-free CRISPR-Cas9 RNP-mediated mutagenesis. *Biotechnol. Bioeng.* 115:719–728. doi:10.1002/bit.26499.

Baladehi, M.H., M. Hekmatara, Y. He, Y. Bhaskar, Z. Wang, L. Liu, Y. Ji, and J. Xu. 2021. Culture-free identification and metabolic profiling of microalgal single cells via ensemble learning of ramanomes. *Anal. Chem.* doi:10.1021/acs.analchem.1c01015.

Ball, S.G. 2002. The Intricate Pathway of Starch Biosynthesis and Degradation in the Monocellular Alga *Chlamydomonas reinhardtii*. *Aust. J. Chem.* 55:49–59.

Ball, S.G., and P. Deschamps. 2009. Starch Metabolism. *Chlamydomonas Sourceb. 3-Vol set*. 2:1–40. doi:10.1016/B978-0-12-370873-1.00009-5.

Banerjee, S., A. Ray, and D. Das. 2021. Optimization of *Chlamydomonas reinhardtii* cultivation with simultaneous CO_2 sequestration and biofuels production in a biorefinery framework. *Sci. Total Environ.* 762:143080. doi:10.1016/j.scitotenv.2020.143080.

Baumeister, T.U.H., M. Vallet, F. Kaftan, A. Svatoš, and G. Pohnert. 2019. Live single-cell metabolomics with matrix-free laser/desorption ionization mass spectrometry to address microalgal physiology. *Front. Plant Sci.* 10:1–9. doi:10.3389/fpls.2019.00172.

Bazzani, E., C. Lauritano, O. Mangoni, F. Bolinesi, and M. Saggiomo. 2021. *Chlamydomonas* responses to salinity stress and possible biotechnological exploitation. *J. Mar. Sci. Eng.* 9. doi:10.3390/jmse9111242.

Behrendt, L., M. Mehdi Salek, E.L. Trampe, V.I. Fernandez, K.S. Lee, M. Kühl, and R. Stocker. 2020. PhenoChip: A single-cell phenomic platform for highthroughput photophysiological analyses of microalgae. *Sci. Adv.* 6:1–14. doi:10.1126/sciadv.abb2754.

Benavente-Valdés, J.R., C. Aguilar, J.C. Contreras-Esquivel, A. Méndez-Zavala, and J. Montañez. 2016. Strategies to enhance the production of photosynthetic pigments and lipids in chlorophycae species. *Biotechnol. Reports*. 10:117–125. doi:10.1016/j.btre.2016.04.001.

Benvenuti, G., R. Bosma, F. Ji, P. Lamers, M.J. Barbosa, and R.H. Wijffels. 2016. Batch and semi-continuous microalgal TAG production in lab-scale and outdoor photobioreactors. *J. Appl. Phycol.* 28:3167–3177. doi:10.1007/s10811-016-0897-1.

Bertozzini, E., L. Galluzzi, A. Penna, and M. Magnani. 2011. Application of the standard addition method for the absolute quantification of neutral lipids in microalgae using Nile red. *J. Microbiol. Methods*. 87:17–23. doi:10.1016/j.mimet.2011.06.018.

Bhattacharya, S., R. Maurya, S. Kumar, and T. Ghosh. 2016. Solar driven mass cultivation and the extraction of lipids from *Chlorella variabilis* : A case study. *ALGAL*. 14:137–142. doi:10.1016/j.algal.2016.01.009.

Bisht, B., V. Kumar, P. Gururani, M.S. Tomar, M. Nanda, M.S. Vlaskin, S. Kumar, and A. Kurbatova. 2021. The potential of nuclear magnetic resonance (NMR) in metabolomics and lipidomics of microalgae- a review. *Arch. Biochem. Biophys.* 710:108987. doi:10.1016/j.abb.2021.108987.

Blaby, I.K., A.G. Glaesener, T. Mettler, S.T. Fitz-Gibbon, S.D. Gallaher, B. Liu, N.R. Boyle, J. Kropat, M. Stitt, S. Johnson, C. Benning, M. Pellegrini, D. Casero, and S.S. Merchant. 2013. Systems-level analysis of nitrogen starvation-induced modifications of carbon metabolism in a *Chlamydomonas reinhardtii* starchless mutant. *Plant Cell*. 25:4305–4323. doi:10.1105/tpc.113.117580.

Black, S.K., S.L. Smolinski, C. Feehan, P.T. Pienkos, E.E. Jarvis, and L.M.L. Laurens. 2013. New method for discovery of starch phenotypes in growing microalgal colonies. *Anal. Biochem.* 432:71–73. doi:10.1016/j.ab.2012.09.018.

Boyle, N.R., and J.A. Morgan. 2009. Flux balance analysis of primary metabolism in *Chlamydomonas reinhardtii*. *BMC Syst. Biol.* 3:1–14. doi:10.1186/1752-0509-3-4.

Boyle, N.R., M.D. Page, B. Liu, I.K. Blaby, D. Casero, J. Kropat, S.J. Cokus, A. Hong-Hermesdorf, J. Shaw, S.J. Karpowicz, S.D. Gallaher, S. Johnson, C. Benning, M.

Pellegrini, A. Grossman, and S.S. Merchant. 2012. Three acyltransferases and nitrogen-responsive regulator are implicated in nitrogen starvation-induced triacylglycerol accumulation in *Chlamydomonas*. *J. Biol. Chem.* 287:15811–15825. doi:10.1074/jbc.M111.334052.

Breuer, G., W.A.C. Evers, J.H. de Vree, D.M.M. Kleinegris, D.E. Martens, R.H. Wijffels, and P.P. Lamers. 2013. Analysis of Fatty Acid Content and Composition in Microalgae. *J. Vis. Exp.* 5:1–9. doi:10.3791/50628.

Busi, M. V., J. Barchiesi, M. Martín, and D.F. Gomez-Casati. 2014. Starch metabolism in green algae. *Starch/Staerke*. 66:28–40. doi:10.1002/star.201200211.

Cakmak, T., P. Angun, Y.E. Demiray, A.D. Ozkan, Z. Elibol, and T. Tekinay. 2012. Differential effects of nitrogen and sulfur deprivation on growth and biodiesel feedstock production of *Chlamydomonas reinhardtii*. *Biotechnol. Bioeng.* 109:1947–1957. doi:10.1002/bit.24474.

Calixto, C.D., J.K. da Silva Santana, V.P. Tibúrcio, L. de F.B.L. de Pontes, C.F. da Costa Sassi, M.M. da Conceição, and R. Sassi. 2018. Productivity and fuel quality parameters of lipids obtained from 12 species of microalgae from the northeastern region of Brazil. *Renew. Energy*. 115:1144–1152. doi:10.1016/j.renene.2017.09.029.

Carmo da Silva, J., and A.T. Lombardi. 2020. Chlorophylls in Microalgae: Occurrence, Distribution, and Biosynthesis. *In* Pigments from Microalgae Handbook. 1–18.

de Carvalho Silvello, M.A., I. Severo Gonçalves, S. Patrícia Held Azambuja, S. Silva Costa, P. Garcia Pereira Silva, L. Oliveira Santos, and R. Goldbeck. 2022. Microalgae-based carbohydrates: A green innovative source of bioenergy. *Bioresour. Technol.* 344. doi:10.1016/j.biortech.2021.126304.

Chang, W.C., H.Q. Zheng, and C.N.N. Chen. 2016. Comparative transcriptome analysis reveals a potential photosynthate partitioning mechanism between lipid and starch biosynthetic pathways in green microalgae. *Algal Res.* 16:54–62. doi:10.1016/j.algal.2016.03.007.

Chen, B., C. Wan, M.A. Mehmood, J.S. Chang, F. Bai, and X. Zhao. 2017a. Manipulating environmental stresses and stress tolerance of microalgae for enhanced production of lipids and value-added products–A review. *Bioresour. Technol.* 244:1198–1206. doi:10.1016/j.biortech.2017.05.170.

Chen, H., J. Hu, Y. Qiao, W. Chen, J. Rong, Y. Zhang, C. He, and Q. Wang. 2015. Ca 2+ -regulated cyclic electron flow supplies ATP for nitrogen starvation-induced lipid biosynthesis in green alga. *Sci. Rep.* 5:1–12. doi:10.1038/srep15117.

Chen, H., and Q. Wang. 2021. Regulatory mechanisms of lipid biosynthesis in microalgae. *Biol. Rev.* 96:2373–2391. doi:10.1111/brv.12759.

Chen, J.H., Y. Kato, M. Matsuda, C.Y. Chen, D. Nagarajan, T. Hasunuma, A. Kondo, and J.S. Chang. 2021. Lutein production with *Chlorella sorokiniana* MB-1-M12 using novel two-stage cultivation strategies – metabolic analysis and process improvement. *Bioresour. Technol.* 334:125200. doi:10.1016/j.biortech.2021.125200.

Chen, J.W., W.J. Liu, D.X. Hu, X. Wang, S. Balamurugan, A. Alimujiang, W.D. Yang, J.S. Liu, and H.Y. Li. 2017b. Identification of a malonyl CoA-acyl carrier protein transacylase and its regulatory role in fatty acid biosynthesis in oleaginous microalga *Nannochloropsis oceanica*. *Biotechnol. Appl. Biochem.* 64:620–626. doi:10.1002/bab.1531.

Chen, Y.H., and T.H. Walker. 2011. Biomass and lipid production of heterotrophic

microalgae *Chlorella protothecoides* by using biodiesel-derived crude glycerol. *Biotechnol. Lett.* 33:1973–1983. doi:10.1007/s10529-011-0672-y.

Cheng, D., and Q. He. 2014. Assessment of environmental stresses for enhanced microalgal biofuel production – an overview. 2:1–8. doi:10.3389/fenrg.2014.00026.

Cheng, P., J. Huang, X. Song, T. Yao, J. Jiang, C. Zhou, X. Yan, and R. Ruan. 2022. Heterotrophic and mixotrophic cultivation of microalgae to simultaneously achieve furfural wastewater treatment and lipid production. *Bioresour. Technol.* 349:126888. doi:10.1016/J.BIORTECH.2022.126888.

Choi, Y.E., J.K. Rhee, H.S. Kim, J.W. Ahn, H. Hwang, and J.W. Yang. 2015. Chemical genetics approach reveals importance of cAMP and MAP kinase signaling to lipid and carotenoid biosynthesis in microalgae. *J. Microbiol. Biotechnol.* 25:637–647. doi:10.4014/jmb.1408.08035.

Chokshi, K., I. Pancha, K. Trivedi, B. George, R. Maurya, A. Ghosh, and S. Mishra. 2015. Biofuel potential of the newly isolated microalgae Acutodesmus dimorphus under temperature induced oxidative stress conditions. *Bioresour. Technol.* 180:162–171. doi:10.1016/j.biortech.2014.12.102.

Cordero, B.F., I. Obraztsova, L. Martín, I. Couso, R. León, M. Ángeles Vargas, and H. Rodríguez. 2010. Isolation and characterization of a lycopene β-cyclase gene from the astaxanthin-producing green alga *Chlorella Zofingiensis* (chlorophyta). *J. Phycol.* 46:1229–1238. doi:10.1111/j.1529-8817.2010.00907.x.

Costa, J.A.V., B.C.B. Freitas, G.M. Rosa, L. Moraes, M.G. Morais, and B.G. Mitchell. 2019. Operational and economic aspects of Spirulina-based biorefinery. *Bioresour. Technol.* 292:121946. doi:10.1016/j.biortech.2019.121946.

Couso, I., and J.L. Crespo. 2017. The TOR Signaling Network in the Model Unicellular Green Alga *Chlamydomonas reinhardtii*. *Biomolecules*. 7:54. doi:10.3390/biom7030054.

Couso, I., M.E. Pérez-Pérez, E. Martínez-Force, H.-S. Kim, Y. He, J.G. Umen, J.L. Crespo, and P. Bozhkov. 2017. Autophagic flux is required for the synthesis of triacylglycerols and ribosomal protein turnover in *Chlamydomonas*. *J. Exp. Bot.* doi:10.1093/jxb/erx372.

Dao, G.H., G.X. Wu, X.X. Wang, L.L. Zhuang, T.Y. Zhang, and H.Y. Hu. 2018. Enhanced growth and fatty acid accumulation of microalgae *Scenedesmus* sp. LX1 by two types of auxin. *Bioresour. Technol.* 247:561–567. doi:10.1016/j.biortech.2017.09.079.

Das, A.A.K., M.M.N. Esfahani, O.D. Velev, N. Pamme, and V.N. Paunov. 2015. Artificial leaf device for hydrogen generation from immobilised *C. reinhardtii* microalgae. *J. Mater. Chem. A.* 3:20698–20707. doi:10.1039/c5ta07112g.

Datta, A., A. Hossain, and S. Roy. 2019. An overview on biofuels and their advantages and disadvantages. *Asian J. Chem.* 31:1851–1858. doi:10.14233/ajchem.2019.22098.

Davey, M.P., I. Horst, G.H. Duong, E. V. Tomsett, A.C.P. Litvinenko, C.J. Howe, and A.G. Smith. 2014. Triacylglyceride Production and Autophagous Responses in *Chlamydomonas reinhardtii* Depend on Resource Allocation and Carbon Source. *Eukaryot. Cell*. 13:392–400. doi:10.1128/EC.00178-13.

Davis, R.W., H.D.T. Jones, A.M. Collins, J.B. Ricken, M.B. Sinclair, J.A. Timlin, and S. Singh. 2014. Label-free measurement of algal triacylglyceride production using fluorescence hyperspectral imaging. *Algal Res.* 5:181–189. doi:10.1016/j.algal.2013.11.010.

Dębowski, M., M. Zieliński, J. Kazimierowicz, N. Kujawska, and S. Talbierz. 2020.

Microalgae cultivation technologies as an opportunity for bioenergetic system development—advantages and limitations. *Sustain.* 12:1–37. doi:10.3390/su12239980.

Demir-Yilmaz, I., P. Guiraud, and C. Formosa-Dague. 2021. The contribution of Atomic Force Microscopy (AFM) in microalgae studies: A review. *Algal Res.* 60:1–17. doi:10.1016/j.algal.2021.102506.

Engel, B.D., M. Schaffer, L.K. Cuellar, E. Villa, J.M. Plitzko, and W. Baumeister. 2015. Native architecture of the *Chlamydomonas* chloroplast revealed by in situ cryo-electron tomography. *Elife*. 2015:1–29. doi:10.7554/eLife.04889.

Erickson, E., S. Wakao, and K.K. Niyogi. 2015. Light stress and photoprotection in *Chlamydomonas reinhardtii*. *Plant J.* 82:449–465. doi:10.1111/tpj.12825.

Fan, J., C. Andre, and C. Xu. 2011. A chloroplast pathway for the de novo biosynthesis of triacylglycerol in *Chlamydomonas reinhardtii*. *FEBS Lett.* 585:1985–1991. doi:10.1016/j.febslet.2011.05.018.

Fan, J., C. Yan, C. Andre, J. Shanklin, J. Schwender, and C. Xu. 2012. Oil accumulation is controlled by carbon precursor supply for fatty acid synthesis in *Chlamydomonas reinhardtii*. *Plant Cell Physiol.* 53:1380–1390. doi:10.1093/pcp/pcs082.

Ferreira, V.S., R.F. Pinto, and C. Sant'Anna. 2016. Low light intensity and nitrogen starvation modulate the chlorophyll content of *Scenedesmus dimorphus*. *J. Appl. Microbiol.* 120:661–670. doi:10.1111/jam.13007.

Fields, F.J., J.T. Ostrand, and S.P. Mayfield. 2018. Fed-batch mixotrophic cultivation of *Chlamydomonas reinhardtii* for high-density cultures. *Algal Res.* 33:109–117. doi:10.1016/j.algal.2018.05.006.

Gala de Pablo, J., M. Lindley, K. Hiramatsu, A. Isozaki, and K. Goda. 2023. Label-free live microalgal starch screening via Raman flow cytometry. *Algal Res.* 70:102993. doi:https://doi.org/10.1016/j.algal.2023.102993.

Gallego-Cartagena, E., M. Castillo-Ramírez, and W. Martínez-Burgos. 2019. Effect of stressful conditions on the carotenogenic activity of a Colombian strain of *Dunaliella salina*. *Saudi J. Biol. Sci.* 26:1325–1330. doi:10.1016/j.sjbs.2019.07.010.

Ganesan, R., S. Manigandan, M.S. Samuel, R. Shanmuganathan, K. Brindhadevi, N.T. Lan Chi, P.A. Duc, and A. Pugazhendhi. 2020. A review on prospective production of biofuel from microalgae. *Biotechnol. Reports*. 27:e00509. doi:10.1016/j.btre.2020.e00509.

Gardner, R., P. Peters, B. Peyton, and K.E. Cooksey. 2011. Medium pH and nitrate concentration effects on accumulation of triacylglycerol in two members of the chlorophyta. *J. Appl. Phycol.* 23:1005–1016. doi:10.1007/s10811-010-9633-4.

Gong, M., and A. Bassi. 2016. Carotenoids from microalgae: A review of recent developments. *Biotechnol. Adv.* 34:1396–1412. doi:10.1016/j.biotechadv.2016.10.005.

Goodenough, U., I. Blaby, D. Casero, S.D. Gallaher, C. Goodson, S. Johnson, J.H. Lee, S.S. Merchant, M. Pellegrini, R. Roth, J. Rusch, M. Singh, J.G. Umen, T.L. Weiss, and T. Wulan. 2014. The path to triacylglyceride obesity in the sta6 strain of *Chlamydomonas reinhardtii*. *Eukaryot. Cell*. 13:591–613. doi:10.1128/EC.00013-14.

Goold, H., F. Beisson, G. Peltier, and Y. Li-Beisson. 2015. Microalgal lipid droplets: composition, diversity, biogenesis and functions. *Plant Cell Rep.* 34:545–555. doi:10.1007/s00299-014-1711-7.

Greenspan, P., E.P. Mayer, and S.D. Fowler. 1985. Nile red: A selective fluorescent stain for

intracellular lipid droplets. *J. Cell Biol.* 100:965–973. doi:10.1083/jcb.100.3.965.

Guan, M., M. Wang, K. Zhanghao, X. Zhang, M. Li, W. Liu, J. Niu, X. Yang, L. Chen, Z. Jing, M.Q. Zhang, D. Jin, P. Xi, and J. Gao. 2022. Polarization modulation with optical lock-in detection reveals universal fluorescence anisotropy of subcellular structures in live cells. *Light Sci. Appl.* 11:1–13. doi:10.1038/s41377-021-00689-1.

Guidetti Vendruscolo, R., M. Bittencourt Fagundes, E. Jacob-Lopes, and R. Wagner. 2019. Analytical strategies for using gas chromatography to control and optimize microalgae bioprocessing. *Curr. Opin. Food Sci.* 25:73–81. doi:10.1016/j.cofs.2019.02.008.

Harun, R., M. Singh, G.M. Forde, and M.K. Danquah. 2010. Bioprocess engineering of microalgae to produce a variety of consumer products. *Renew. Sustain. Energy Rev.* 14:1037–1047. doi:10.1016/j.rser.2009.11.004.

Hayashi, Y., N. Sato, A. Shinozaki, and M. Watanabe. 2015. Increase in peroxisome number and the gene expression of putative glyoxysomal enzymes in *Chlamydomonas* cells supplemented with acetate. *J. Plant Res.* 128:177–185. doi:10.1007/s10265-014-0681-8.

He, M., Y. Yan, F. Pei, M. Wu, T. Gebreluel, S. Zou, and C. Wang. 2017a. Improvement on lipid production by *Scenedesmus obliquus* triggered by low dose exposure to nanoparticles. *Sci. Rep.* 7:1–12. doi:10.1038/s41598-017-15667-0.

He, Q., H. Yang, L. Wu, and C. Hu. 2015. Effect of light intensity on physiological changes, carbon allocation and neutral lipid accumulation in oleaginous microalgae. *Bioresour. Technol.* 191:219–228. doi:10.1016/j.biortech.2015.05.021.

He, Y., P. Zhang, S. Huang, T. Wang, Y. Ji, and J. Xu. 2017b. Label-free, simultaneous quantification of starch, protein and triacylglycerol in single microalgal cells. *Biotechnol Biofuels*. 10:1–18. doi:10.1186/s13068-017-0967-x.

Heredia, V., O. Gonçalves, L. Marchal, and J. Pruvost. 2021. Producing energy-rich microalgae biomass for liquid biofuels: Influence of strain selection and culture conditions. *Energies*. 14. doi:10.3390/en14051246.

Hildebrandt, T.M., A. Nunes Nesi, W.L. Araújo, and H.P. Braun. 2015. Amino Acid Catabolism in Plants. *Mol. Plant*. 8:1563–1579. doi:10.1016/j.molp.2015.09.005.

Ho, D.P., H.H. Ngo, and W. Guo. 2014a. A mini review on renewable sources for biofuel. *Bioresour. Technol.* 169:742–749. doi:10.1016/j.biortech.2014.07.022.

Ho, S.H., A. Nakanishi, X. Ye, J.S. Chang, K. Hara, T. Hasunuma, and A. Kondo. 2014b. Optimizing biodiesel production in marine *Chlamydomonas* sp. JSC4 through metabolic profiling and an innovative salinity-gradient strategy. *Biotechnol. Biofuels*. 7:1–16. doi:10.1186/1754-6834-7-97.

Hounslow, E., J. Noirel, D.J. Gilmour, and P.C. Wright. 2017. Lipid quantification techniques for screening oleaginous species of microalgae for biofuel production. *Eur. J. Lipid Sci. Technol.* 119. doi:10.1002/ejlt.201500469.

Huang, Y.Y., C.M. Beal, W.W. Cai, R.S. Ruoff, and E.M. Terentjev. 2010. Micro-Raman spectroscopy of algae: Composition analysis and fluorescence background behavior. *Biotechnol. Bioeng.* 105:889–898. doi:10.1002/bit.22617.

Iasimone, F., A. Panico, V. De Felice, F. Fantasma, M. Iorizzi, and F. Pirozzi. 2018. Effect of light intensity and nutrients supply on microalgae cultivated in urban wastewater: Biomass production, lipids accumulation and settleability characteristics. *J. Environ. Manage.* 223:1078–1085. doi:10.1016/j.jenvman.2018.07.024.

Jaeger, D., C. Pilger, H. Hachmeister, E. Oberländer, R. Wördenweber, J. Wichmann, J.H.

Mussgnug, T. Huser, and O. Kruse. 2016. Label-free in vivo analysis of intracellular lipid droplets in the oleaginous microalga *Monoraphidium neglectum* by coherent Raman scattering microscopy. *Sci. Rep.* 6:2–10. doi:10.1038/srep35340.

James, G.O., C.H. Hocart, W. Hillier, H. Chen, F. Kordbacheh, G.D. Price, and M.A. Djordjevic. 2011. Fatty acid profiling of *Chlamydomonas reinhardtii* under nitrogen deprivation. *Bioresour. Technol.* 102:3343–3351. doi:10.1016/j.biortech.2010.11.051.

Jia, J., D. Han, H.G. Gerken, Y. Li, M. Sommerfeld, Q. Hu, and J. Xu. 2015. Molecular mechanisms for photosynthetic carbon partitioning into storage neutral lipids in *Nannochloropsis oceanica* under nitrogen-depletion conditions. *Algal Res.* 7:66–77. doi:10.1016/j.algal.2014.11.005.

Jiao, Y., H.L. Ouyang, Y.J. Jiang, X.Z. Kong, W. He, W.X. Liu, B. Yang, and F.L. Xu. 2017. Effects of phosphorus stress on the photosynthetic and physiological characteristics of *Chlorella vulgaris* based on chlorophyll fluorescence and flow cytometric analysis. *Ecol. Indic.* 78:131–141. doi:10.1016/J.ECOLIND.2017.03.010.

Johnson, X., and J. Alric. 2013. Central carbon metabolism and electron transport in *Chlamydomonas reinhardtii*: Metabolic constraints for carbon partitioning between oil and starch. *Eukaryot. Cell*. 12:776–793. doi:10.1128/EC.00318-12.

Karpf, S., C. Riche, D. di Carlo, A. Goel, W.A. Zeiger, A. Suresh, C. Portera-Cailliau, and B. Jalali. 2017. Spectro-temporal encoded Multiphoton Microscopy. *arXiv*. 1–21.

Khanra, S., M. Mondal, G. Halder, O.N. Tiwari, K. Gayen, and T.K. Bhowmick. 2018. Downstream processing of microalgae for pigments, protein and carbohydrate in industrial application: A review. *Food Bioprod. Process.* 110:60–84. doi:10.1016/j.fbp.2018.02.002.

Khoeyi, Z.A., J. Seyfabadi, and Z. Ramezanpour. 2012. Effect of light intensity and photoperiod on biomass and fatty acid composition of the microalgae, *Chlorella vulgaris*. *Aquac. Int.* 20:41–49. doi:10.1007/s10499-011-9440-1.

Khoo, K.S., S.Y. Lee, C.W. Ooi, X. Fu, X. Miao, T.C. Ling, and P.L. Show. 2019. Recent advances in biorefinery of astaxanthin from *Haematococcus pluvialis*. *Bioresour. Technol.* 288:121606. doi:10.1016/j.biortech.2019.121606.

Kim, H.S., T.P. Devarenne, and A. Han. 2018. Microfluidic systems for microalgal biotechnology: A review. *Algal Res.* 30:149–161. doi:10.1016/j.algal.2017.11.020.

Kim, H.S., S.C. Hsu, S.I. Han, H.R. Thapa, A.R. Guzman, D.R. Browne, M. Tatli, T.P. Devarenne, D.B. Stern, and A. Han. 2017. High-throughput droplet microfluidics screening platform for selecting fast-growing and high lipid-producing microalgae from a mutant library. *Plant Direct*. 1. doi:10.1002/pld3.11.

Kim, S., H. Kim, D. Ko, Y. Yamaoka, M. Otsuru, M. Kawai-Yamada, T. Ishikawa, H.M. Oh, I. Nishida, Y. Li-Beisson, and Y. Lee. 2013. Rapid induction of lipid droplets in *Chlamydomonas reinhardtii* and *Chlorella vulgaris* by Brefeldin a. *PLoS One*. 8. doi:10.1371/journal.pone.0081978.

Kong, F., I.T. Romero, Y. Li-beisson, and J. Warakanont. 2018. Lipid catabolism in microalgae. doi:10.1111/nph.15047.

Kumar, G., S.H. Kim, C.H. Lay, and V.K. Ponnusamy. 2020. Recent developments on alternative fuels, energy and environment for sustainability. *Bioresour. Technol.* 317:2019–2021. doi:10.1016/j.biortech.2020.124010.

Kumar, M., M.P. Sharma, and G. Dwivedi. 2013. Algae Oil as Future Energy Source in Indian Perspective. *Int. J. Renew. ENERGY Res.* 3:913–921.

Lee, D.H., C.Y. Bae, J.I. Han, and J.K. Park. 2013a. In situ analysis of heterogeneity in the lipid content of single green microalgae in alginate hydrogel microcapsules. *Anal. Chem.* 85:8749–8756. doi:10.1021/ac401836j.

Lee, J., Y. Yamaoka, F. Kong, C. Cagnon, A. Beyly-Adriano, S. Jang, P. Gao, B.H. Kang, Y. Li-Beisson, and Y. Lee. 2020. The phosphatidylethanolamine-binding protein DTH1 mediates degradation of lipid droplets in *Chlamydomonas reinhardtii*. *Proc. Natl. Acad. Sci. U. S. A.* 117:23131–23139. doi:10.1073/pnas.2005600117.

Lee, R.A., and J.M. Lavoie. 2013. From first- to third-generation biofuels: Challenges of producing a commodity from a biomass of increasing complexity. *Anim. Front.* 3:6–11. doi:10.2527/af.2013-0010.

Lee, T., J. Chang, and H. Wang. 2013b. Current developments in high-throughput analysis for microalgae cellular contents. *Biotechnol. J.* 8:1301–1314. doi:10.1002/biot.201200391.

Lee, T.H., J.S. Chang, and H.Y. Wang. 2013c. Rapid and in vivo quantification of cellular lipids in *Chlorella vulgaris* using near-infrared Raman spectrometry. *Anal. Chem.* 85:2155–2160. doi:10.1021/ac3028118.

Lee, T.M., J.Y. Lin, T.H. Tsai, R.Y. Yang, and I.S. Ng. 2023. Clustered regularly interspaced short palindromic repeats (CRISPR) technology and genetic engineering strategies for microalgae towards carbon neutrality: A critical review. *Bioresour. Technol.* 368:128350. doi:10.1016/J.BIORTECH.2022.128350.

Levasseur, W., P. Perré, and V. Pozzobon. 2020. A review of high value-added molecules production by microalgae in light of the classification. *Biotechnol. Adv.* 41:107545. doi:10.1016/j.biotechadv.2020.107545.

Li-Beisson, Y., F. Beisson, and W. Riekhof. 2015. Metabolism of acyl-lipids in *Chlamydomonas reinhardtii*. *Plant J.* 82:504–522. doi:10.1111/tpj.12787.

Li-Beisson, Y., F. Kong, P. Wang, Y. Lee, and B.H. Kang. 2021. The disassembly of lipid droplets in *Chlamydomonas*. *New Phytol.* 231:1359–1364. doi:10.1111/nph.17505.

Li-Beisson, Y., J.J. Thelen, E. Fedosejevs, and J.L. Harwood. 2019. The lipid biochemistry of eukaryotic algae. *Prog. Lipid Res.* 74:31–68. doi:10.1016/j.plipres.2019.01.003.

Li, X., E.R. Moellering, B. Liu, C. Johnny, M. Fedewa, B.B. Sears, M.H. Kuo, and C. Benning. 2012. A galactoglycerolipid lipase is required for triacylglycerol accumulation and survival following nitrogen deprivation in *Chlamydomonas reinhardtii* c w. *Plant Cell*. 24:4670–4686. doi:10.1105/tpc.112.105106.

Li, Y., D. Han, M. Sommerfeld, and Q. Hu. 2011. Photosynthetic carbon partitioning and lipid production in the oleaginous microalga *Pseudochlorococcum* sp. (Chlorophyceae) under nitrogen-limited conditions. *Bioresour. Technol.* 102:123–129. doi:10.1016/j.biortech.2010.06.036.

Li, Y., M. Horsman, N. Wu, C.Q. Lan, and N. Dubois-Calero. 2008. Biofuels from microalgae. *Biotechnol. Prog.* 24:815–820. doi:10.1021/bp.070371k.

Li, Y., H. Xu, F. Han, J. Mu, D. Chen, B. Feng, and H. Zeng. 2014. Regulation of lipid metabolism in the green microalga *Chlorella protothecoides* by heterotrophy-photoinduction cultivation regime. *Bioresour. Technol.* 192:781–791. doi:10.1016/j.biortech.2014.07.028.

Lian, L., X. Hu, Z. Huang, L. Hu, and L. Xu. 2021. Pigment analysis based on a line-scanning fluorescence hyperspectral imaging microscope combined with multivariate curve resolution. *PLoS One*. 16:1–14. doi:10.1371/journal.pone.0254864.

Liang, Y., N. Sarkany, and Y. Cui. 2009. Biomass and lipid productivities of Chlorella vulgaris under autotrophic, heterotrophic and mixotrophic growth conditions. *Biotechnol. Lett.* 31:1043–1049. doi:10.1007/s10529-009-9975-7.

Lichtenthaler, H.K., C. Buschmann, and M. Knapp. 2005. Chlorophylls and carotenoids: Measurements and characterization by UV-Vis spectroscopy. *Photosynthetica*. 43:379–393. doi:10.1007/s11099-005-0062-6.

Lidstrom, M.E., and M.C. Konopka. 2010. The role of physiological heterogeneity in microbial population behavior. *Nat. Chem. Biol.* 6:705–712. doi:10.1038/nchembio.436.

Lin, T.S., and J.Y. Wu. 2015. Effect of carbon sources on growth and lipid accumulation of newly isolated microalgae cultured under mixotrophic condition. *Bioresour. Technol.* 184:100–107. doi:10.1016/j.biortech.2014.11.005.

Liu, B., and C. Benning. 2013. Lipid metabolism in microalgae distinguishes itself. *Curr. Opin. Biotechnol.* 24:300–309. doi:10.1016/j.copbio.2012.08.008.

Liu, J.Y., L.H. Zeng, and Z.H. Ren. 2020. Recent application of spectroscopy for the detection of microalgae life information: A review. *Appl. Spectrosc. Rev.* 55:26–59. doi:10.1080/05704928.2018.1509345.

Liu, X., and Christopher Q. Lan. 2014. Quantitative Determination of Lipid Analysis Using Nile Red Fluorometry. Master Deg:113.

Liyanaarachchi, V.C., M. Premaratne, T.U. Ariyadasa, P.H.V. Nimarshana, and A. Malik. 2021. Two-stage cultivation of microalgae for production of high-value compounds and biofuels: A review. *Algal Res.* 57:102353. doi:10.1016/j.algal.2021.102353.

Long, S.F., S. Kang, Q.Q. Wang, Y.T. Xu, L. Pan, J.X. Hu, M. Li, and X.S. Piao. 2018. Dietary supplementation with DHA-rich microalgae improves performance, serum composition, carcass trait, antioxidant status, and fatty acid profile of broilers. *Poult. Sci.* 97:1881–1890. doi:10.3382/ps/pey027.

Lu, H., K. Liu, H. Zhang, X. Xie, Y. Ge, Z. Chi, S. Xue, F. Kong, and T. Ohama. 2023. Enhanced triacyclglycerols and starch synthesis in *Chlamydomonas* stimulated by the engineered biodegradable nanoparticles. *Appl. Microbiol. Biotechnol.* 107:971–983. doi:10.1007/s00253-023-12366-x.

Ma, R., Z. Zhang, S.H. Ho, C. Ruan, J. Li, Y. Xie, X. Shi, L. Liu, and J. Chen. 2020. Two-stage bioprocess for hyper-production of lutein from microalga *Chlorella sorokiniana* FZU60: Effects of temperature, light intensity, and operation strategies. *Algal Res.* 52:102119. doi:10.1016/j.algal.2020.102119.

Maneechote, W., and B. Cheirsilp. 2021. Stepwise-incremental physicochemical factors induced acclimation and tolerance in oleaginous microalgae to crucial outdoor stresses and improved properties as biodiesel feedstocks. *Bioresour. Technol.* 328:124850. doi:10.1016/j.biortech.2021.124850.

Marquez, V., and A. Beccaria. 2020. Application of Oil Red O staining in oleaginous microalgae: practical uses in screening and lipid quantification of different species. *J. Appl. Phycol.* 32:1755–1761. doi:10.1007/s10811-020-02098-0.

Martins, B.M.C., and J.C.W. Locke. 2015. Microbial individuality: how single-cell heterogeneity enables population level strategies. *Curr. Opin. Microbiol.* 24:104–112. doi:10.1016/j.mib.2015.01.003.

Mat Aron, N.S., K.S. Khoo, K.W. Chew, P.L. Show, W.H. Chen, and T.H.P. Nguyen. 2020. Sustainability of the four generations of biofuels – A review. *Int. J. Energy Res.* 44:9266–9282. doi:10.1002/er.5557.

Mendes, A., T.L. Da Silva, and A. Reis. 2007. DHA concentration and purification from the marine heterotrophic microalga *Crypthecodinium cohnii* CCMP 316 by winterization and urea complexation. *Food Technol. Biotechnol.* 45:38–44.

Merchant, S.S., S.E. Prochnik, and O. et al. Vallon. 2007. The *Chlamydomonas* genome reveals the evolution of key animal and plant functions. *Science (80-.).* 318:245–250. doi:10.1126/science.1143609.

Miao, X., and Q. Wu. 2006. Biodiesel production from heterotrophic microalgal oil. *Bioresour. Technol.* 97:841–846. doi:10.1016/j.biortech.2005.04.008.

Minyuk, G., R. Sidorov, and A. Solovchenko. 2020. Effect of nitrogen source on the growth, lipid, and valuable carotenoid production in the green microalga *Chromochloris zofingiensis*. *J. Appl. Phycol.* 32:923–935. doi:10.1007/s10811-020-02060-0.

Mirizadeh, S., M. Nosrati, and S.A. Shojaosadati. 2020. Synergistic Effect of Nutrient and Salt Stress on Lipid Productivity of *Chlorella vulgaris* Through Two-Stage Cultivation. *Bioenergy Res.* 13:507–517. doi:10.1007/s12155-019-10077-8.

Missoum, A. 2019. a Mini-Review on Biofuels From *Chlamydomonas Reinhardtii*. *J. Microbiol. Biotechnol. Food Sci.* 9:273–279. doi:10.15414/jmbfs.2019.9.2.273-279.

Mobin, S., and F. Alam. 2017. Some Promising Microalgal Species for Commercial Applications: A review. *Energy Procedia*. 110:510–517. doi:10.1016/j.egypro.2017.03.177.

Moon, M., C.W. Kim, W.K. Park, G. Yoo, Y.E. Choi, and J.W. Yang. 2013. Mixotrophic growth with acetate or volatile fatty acids maximizes growth and lipid production in *Chlamydomonas reinhardtii*. *Algal Res.* 2:352–357. doi:10.1016/j.algal.2013.09.003.

Morales-Sanchez, D., Y. Kim, E.L. Terng, L. Peterson, and H. Cerutti. 2017. A multidomain enzyme with glycerol-3-phosphate dehydrogenase and phosphatase.pdf. *Plant J.* 90:1079–1092. doi:10.1111/tpj.13530.

Msanne, J., J. Polle, and S. Starkenburg. 2020. An assessment of heterotrophy and mixotrophy in Scenedesmus and its utilization in wastewater treatment. *Algal Res.* 48:101911. doi:10.1016/j.algal.2020.101911.

Nayak, M., W.I. Suh, Y.K. Chang, and B. Lee. 2019. Exploration of two-stage cultivation strategies using nitrogen starvation to maximize the lipid productivity in *Chlorella* sp. HS2. *Bioresour. Technol.* 276:110–118. doi:10.1016/j.biortech.2018.12.111.

Nekvapil, F., I. Brezestean, G. Lazar, C. Firta, and S.C. Pinzaru. 2022. Resonance Raman and SERRS of fucoxanthin: Prospects for carotenoid quantification in live diatom cells. *J. Mol. Struct.* 1250:131608. doi:https://doi.org/10.1016/j.molstruc.2021.131608.

NGUYEN, H.T. Do, A. RAMLI, and L.M. KEE. 2017. A Review on Methods Used in Analysis of Microalgae Lipid Composition. *J. Japan Inst. Energy*. 96:532–537. doi:10.3775/jie.96.532.

Osterrothová, K., A. Culka, K. Němečková, D. Kaftan, L. Nedbalová, L. Procházková, and J. Jehlička. 2019. Analyzing carotenoids of snow algae by Raman microspectroscopy and high-performance liquid chromatography. *Spectrochim. Acta - Part A Mol. Biomol. Spectrosc.* 212:262–271. doi:10.1016/j.saa.2019.01.013.

Paliwal, C., M. Mitra, K. Bhayani, S.V.V. Bharadwaj, T. Ghosh, S. Dubey, and S. Mishra. 2017. Abiotic stresses as tools for metabolites in microalgae. *Bioresour. Technol.* 244:1216–1226. doi:10.1016/j.biortech.2017.05.058.

Pancha, I., K. Chokshi, T. Ghosh, C. Paliwal, R. Maurya, and S. Mishra. 2015a. Bicarbonate

supplementation enhanced biofuel production potential as well as nutritional stress mitigation in the microalgae *Scenedesmus* sp. CCNM 1077. *Bioresour. Technol.* 193:315–323. doi:10.1016/j.biortech.2015.06.107.

Pancha, I., K. Chokshi, R. Maurya, K. Trivedi, S.K. Patidar, A. Ghosh, and S. Mishra. 2015b. Salinity induced oxidative stress enhanced biofuel production potential of microalgae *Scenedesmus* sp. CCNM 1077. *Bioresour. Technol.* 189:341–348. doi:10.1016/j.biortech.2015.04.017.

Park, W.K., M. Moon, M.S. Kwak, S. Jeon, G.G. Choi, J.W. Yang, and B. Lee. 2014. Use of orange peel extract for mixotrophic cultivation of *Chlorella vulgaris*: Increased production of biomass and FAMEs. *Bioresour. Technol.* 171:343–349. doi:10.1016/j.biortech.2014.08.109.

Patel, A., I. Antonopoulou, J. Enman, U. Rova, P. Christakopoulos, and L. Matsakas. 2019. Lipids detection and quantification in oleaginous microorganisms: an overview of the current state of the art. *BMC Chem. Eng.* 1. doi:10.1186/s42480-019-0013-9.

Patel, A.K., Y.Y. Choi, and S.J. Sim. 2020. Emerging prospects of mixotrophic microalgae: Way forward to sustainable bioprocess for environmental remediation and cost-effective biofuels. *Bioresour. Technol.* 300:122741. doi:10.1016/j.biortech.2020.122741.

Patras, D., C. V. Moraru, and C. Socaciu. 2018. Screening of bioactive compounds synthesized by microalgae: A progress overview on extraction and chemical analysis. *Stud. Univ. Babes-Bolyai Chem.* 63:21–35. doi:10.24193/subbchem.2018.1.02.

Paul, A., Y. Wang, C. Brännmark, S. Kumar, M. Bonn, and S.H. Parekh. 2019. Quantitative Mapping of Triacylglycerol Chain Length and Saturation Using Broadband CARS Microscopy. *Biophys. J.* 116:2346–2355. doi:10.1016/j.bpj.2019.04.036.

Perez-Garcia, O., and Y. Bashan. 2015. Algal biorefineries: Volume 2: Products and refinery design. 1–557 pp.

Perez-Garcia, O., F.M.E. Escalante, L.E. de-Bashan, and Y. Bashan. 2011. Heterotrophic cultures of microalgae: Metabolism and potential products. *Water Res.* 45:11–36. doi:10.1016/j.watres.2010.08.037.

Perez-Martin, M., M.E. Perez-Perez, S.D. Lemaire, and J.L. Crespo. 2014. Oxidative Stress Contributes to Autophagy Induction in Response to Endoplasmic Reticulum Stress in *Chlamydomonas reinhardtii*. *Plant Physiol.* 166:997–1008. doi:10.1104/pp.114.243659.

Pérez-Pérez, M., I. Couso, L. Heredia-Martínez, and J. Crespo. 2017a. Monitoring Autophagy in the Model Green Microalga *Chlamydomonas reinhardtii*. *Cells*. 6:36. doi:10.3390/cells6040036.

Pérez-Pérez, M.E., I. Couso, and J.L. Crespo. 2012. Carotenoid deficiency triggers autophagy in the model green alga *Chlamydomonas reinhardtii*. *Autophagy*. 8:376–388. doi:10.4161/auto.8.3.18864.

Pérez-Pérez, M.E., I. Couso, and J.L. Crespo. 2017b. The TOR signaling network in the model unicellular green alga *Chlamydomonas reinhardtii*. *Biomolecules*. 7:1–13. doi:10.3390/biom7030054.

Perez-Perez, M.E., S.D. Lemaire, and J.L. Crespo. 2012. Reactive Oxygen Species and Autophagy in Plants and Algae. *Plant Physiol.* 160:156–164. doi:10.1104/pp.112.199992.

Phalanisong, P., P. Plangklang, and A. Reungsang. 2021. Photoautotrophic and mixotrophic cultivation of polyhydroxyalkanoate-accumulating microalgae consortia selected under nitrogen and phosphate limitation. *Molecules*. 26. doi:10.3390/molecules26247613.

Prathima Devi, M., G. Venkata Subhash, and S. Venkata Mohan. 2012. Heterotrophic cultivation of mixed microalgae for lipid accumulation and wastewater treatment during sequential growth and starvation phases: Effect of nutrient supplementation. *Renew. Energy*. 43:276–283. doi:10.1016/j.renene.2011.11.021.

Puzanskiy, R., A. Shavarda, D. Romanyuk, and M. Shishova. 2021. The role of trophic conditions in the regulation of physiology and metabolism of *Chlamydomonas reinhardtii* during batch culturing. *J. Appl. Phycol.* 33:2897–2908. doi:10.1007/s10811-021-02510-3.

Rachutin Zalogin, T., and U. Pick. 2014. Inhibition of nitrate reductase by azide in microalgae results in triglycerides accumulation. *Algal Res.* 3:17–23. doi:10.1016/J.ALGAL.2013.11.018.

Ramya, A.N., P.S. Ambily, B.S. Sujitha, M. Arumugam, and K. Kumar. 2017. Single cell lipid pro fi ling of *Scenedesmus quadricauda* CASA-CC202 under nitrogen starved condition by surface enhanced Raman scattering (SERS) fi ngerprinting. 25:200–206. doi:10.1016/j.algal.2017.05.011.

Ran, W., H. Wang, Y. Liu, M. Qi, Q. Xiang, C. Yao, Y. Zhang, and X. Lan. 2019. Storage of starch and lipids in microalgae: Biosynthesis and manipulation by nutrients. *Bioresour. Technol.* 291:121894. doi:10.1016/j.biortech.2019.121894.

Remmers, I.M., A. Hidalgo-Ulloa, B.P. Brandt, W.A.C. Evers, R.H. Wijffels, and P.P. Lamers. 2017. Continuous versus batch production of lipids in the microalgae *Acutodesmus obliquus*. *Bioresour. Technol.* 244:1384–1392. doi:10.1016/j.biortech.2017.04.093.

Rengel, R., R.T. Smith, R.P. Haslam, O. Sayanova, M. Vila, and R. León. 2018. Overexpression of acetyl-CoA synthetase (ACS) enhances the biosynthesis of neutral lipids and starch in the green microalga *Chlamydomonas reinhardtii*. *Algal Res.* 31:183–193. doi:10.1016/j.algal.2018.02.009.

Ribeiro, B.D., D.W. Barreto, and M.A.Z. Coelho. 2011. Technological Aspects of β-Carotene Production. *Food Bioprocess Technol.* 4:693–701. doi:10.1007/s11947-011-0545-3.

Rugnini, L., C. Rossi, S. Antonaroli, A. Rakaj, and L. Bruno. 2020. The influence of light and nutrient starvation on morphology, biomass and lipid content in seven strains of green microalgae as a source of biodiesel. *Microorganisms*. 8:1–13. doi:10.3390/microorganisms8081254.

Rupprecht, J. 2009. From systems biology to fuel-*Chlamydomonas reinhardtii* as a model for a systems biology approach to improve biohydrogen production. *J. Biotechnol.* 142:10–20. doi:10.1016/j.jbiotec.2009.02.008.

Sá, M., N. Ferrer-Ledo, F. Gao, C.G. Bertinetto, J. Jansen, J.G. Crespo, R.H. Wijffels, M. Barbosa, and C.F. Galinha. 2022. Perspectives of fluorescence spectroscopy for online monitoring in microalgae industry. *Microb. Biotechnol.* 15:1824–1838. doi:10.1111/1751-7915.14013.

Saha, S.K., and P. Murray. 2018. Exploitation of microalgae species for nutraceutical purposes: Cultivation aspects. *Fermentation*. 4. doi:10.3390/fermentation4020046.

Sajilata, M.G., R.S. Singhal, and M.Y. Kamat. 2008. Supercritical CO2 extraction of γ-linolenic acid (GLA) from *Spirulina platensis* ARM 740 using response surface methodology. *J. Food Eng.* 84:321–326. doi:10.1016/j.jfoodeng.2007.05.028.

Sajjadi, B., W. Chen, A. Aziz, A. Raman, and S. Ibrahim. 2018. Microalgae lipid and biomass for biofuel production : A comprehensive review on lipid enhancement strategies and

their e ff ects on fatty acid composition. *Renew. Sustain. Energy Rev.* 97:200–232. doi:10.1016/j.rser.2018.07.050.

Sandmann, M., M. Sch, M. Lippold, and S. Rohn. 2018. Analysis of population structures of the microalga *Acutodesmus obliquus* during lipid production using multi-dimensional single-cell analysis. 1–9. doi:10.1038/s41598-018-24638-y.

Sart, S., G. Ronteix, S. Jain, G. Amselem, and C.N. Baroud. 2022. Cell Culture in Microfluidic Droplets. *Chem. Rev.* 122:7061–7096. doi:10.1021/acs.chemrev.1c00666.

Sasso, S., H. Stibor, M. Mittag, and A.R. Grossman. 2018. From molecular manipulation of domesticated *Chlamydomonas reinhardtii* to survival in nature. *Elife*. 7:e39233. doi:10.7554/eLife.39233.

Scaife, M.A., G.T.D.T. Nguyen, J. Rico, D. Lambert, K.E. Helliwell, and A.G. Smith. 2015. Establishing *Chlamydomonas reinhardtii* as an industrial biotechnology host. *Plant J.* 82:532–546. doi:10.1111/tpj.12781.

Schroda, M., D. Hemme, and T. Mühlhaus. 2015. The *Chlamydomonas* heat stress response. *Plant J.* 82:466–480. doi:10.1111/tpj.12816.

Sharma, S.K., D.R. Nelson, R. Abdrabu, B. Khraiwesh, K. Jijakli, M. Arnoux, M.J. O'Connor, T. Bahmani, H. Cai, S. Khapli, R. Jagannathan, and K. Salehi-Ashtiani. 2015. An integrative Raman microscopy-based workflow for rapid in situ analysis of microalgal lipid bodies. *Biotechnol. Biofuels*. 8:1–14. doi:10.1186/s13068-015-0349-1.

Shetty, P., M.M. Gitau, and G. Maróti. 2019. Salinity Stress Responses and Adaptation Mechanisms in Eukaryotic Green Microalgae. *Cells*. 8:1–16. doi:10.3390/cells8121657.

Silva, M.A.A., R.A. Correa, M.G.D.O. Tavares, and N.R. Antoniosi Filho. 2015. A new spectrophotometric method for determination of biodiesel content in biodiesel/diesel blends. *Fuel*. 143:16–20. doi:10.1016/j.fuel.2014.10.048.

da Silva, T.L., P. Moniz, C. Silva, and A. Reis. 2021. The role of heterotrophic microalgae in waste conversion to biofuels and bioproducts. *Processes*. 9:1–24. doi:10.3390/pr9071090.

Skrupski, B., K.E. Wilson, K.L. Goff, and J. Zou. 2013. Effect of pH on neutral lipid and biomass accumulation in microalgal strains native to the Canadian prairies and the Athabasca oil sands. *J. Appl. Phycol.* 25:937–949. doi:10.1007/s10811-012-9930-1.

Smith, R.T., and D.J. Gilmour. 2018. The influence of exogenous organic carbon assimilation and photoperiod on the carbon and lipid metabolism of *Chlamydomonas reinhardtii*. *Algal Res.* 31:122–137. doi:10.1016/j.algal.2018.01.020.

Stančin, H., H. Mikulčić, X. Wang, and N. Duić. 2020. A review on alternative fuels in future energy system. *Renew. Sustain. Energy Rev.* 128. doi:10.1016/j.rser.2020.109927.

Tan, H.L., M.K. Lam, Y.W. Cheng, J.W. Lim, I.S. Tan, C.Y. Henry Foo, and P.L. Show. 2021. Heterotrophic and Mixotrophic Cultivation of *Chlorella vulgaris* using Chicken Waste Compost as Nutrients Source for Lipid Production. *IOP Conf. Ser. Earth Environ. Sci.* 721. doi:10.1088/1755-1315/721/1/012011.

Tan, K.W.M., H. Lin, H. Shen, and Y.K. Lee. 2016. Nitrogen-induced metabolic changes and molecular determinants of carbon allocation in *Dunaliella tertiolecta*. *Sci. Rep.* 6:1–13. doi:10.1038/srep37235.

Tang, D.Y.Y., K.S. Khoo, K.W. Chew, Y. Tao, S.H. Ho, and P.L. Show. 2020. Potential utilization of bioproducts from microalgae for the quality enhancement of natural products. *Bioresour. Technol.* 304:122997. doi:10.1016/j.biortech.2020.122997.

Tarazona Delgado, R., M. dos S. Guarieiro, P.W. Antunes, S.T. Cassini, H.M. Terreros, and V. de O. Fernandes. 2021. Effect of nitrogen limitation on growth, biochemical composition, and cell ultrastructure of the microalga *Picocystis salinarum*. *J. Appl. Phycol.* 33:2083–2092. doi:10.1007/s10811-021-02462-8.

Thurakit, T., W. Pathom-aree, C. Pumas, T.W. Brocklehurst, J. Pekkoh, and S. Srinuanpan. 2022. High-efficiency production of biomass and biofuel under two-stage cultivation of a stable microalga *Botryococcus braunii* mutant generated by ethyl methanesulfonate-induced mutation. *Renew. Energy*. 198:176–188. doi:10.1016/J.RENENE.2022.08.029.

Trampe, E., J. Kolbowski, U. Schreiber, and M. Kühl. 2011. Rapid assessment of different oxygenic phototrophs and single-cell photosynthesis with multicolour variable chlorophyll fluorescence imaging. *Mar. Biol.* 158:1667–1675. doi:10.1007/s00227-011-1663-1.

Tran, Q.G., K. Cho, S. Bin Park, U. Kim, Y.J. Lee, and H.S. Kim. 2019a. Impairment of starch biosynthesis results in elevated oxidative stress and autophagy activity in *Chlamydomonas reinhardtii*. *Sci. Rep.* 9:1–9. doi:10.1038/s41598-019-46313-6.

Tran, Q.G., H.R. Yoon, K. Cho, S.J. Lee, J.L. Crespo, R. Ramanan, and H.S. Kim. 2019b. Dynamic interactions between autophagosomes and lipid droplets in *Chlamydomonas reinhardtii*. *Cells*. 8:7–9. doi:10.3390/cells8090992.

Udayan, A., A.K. Pandey, R. Sirohi, N. Sreekumar, B.I. Sang, S.J. Sim, S.H. Kim, and A. Pandey. 2022. Production of microalgae with high lipid content and their potential as sources of nutraceuticals. *Phytochem. Rev.* 0123456789. doi:10.1007/s11101-021-09784-y.

Valledor, L., T. Furuhashi, A.-M. Hanak, and W. Weckwerth. 2013. Systemic Cold Stress Adaptation of *Chlamydomonas reinhardtii*. *Mol. Cell. Proteomics*. 12:2032–2047. doi:10.1074/mcp.M112.026765.

Veerabadhran, M., S. Natesan, D. MubarakAli, S. Xu, and F. Yang. 2021. Using different cultivation strategies and methods for the production of microalgal biomass as a raw material for the generation of bioproducts. *Chemosphere*. 285:131436. doi:10.1016/j.chemosphere.2021.131436.

Walther, T.C., J. Chung, and R. V. Farese. 2017. Lipid droplet biogenesis. *Annu. Rev. Cell Dev. Biol.* 33:491–510. doi:10.1146/annurev-cellbio-100616-060608.

Wan, M., P. Liu, J. Xia, J.N. Rosenberg, G.A. Oyler, M.J. Betenbaugh, Z. Nie, and G. Qiu. 2011. The effect of mixotrophy on microalgal growth, lipid content, and expression levels of three pathway genes in *Chlorella sorokiniana*. *Appl. Microbiol. Biotechnol.* 91:835–844. doi:10.1007/s00253-011-3399-8.

Wan, M., J. Zhang, D. Hou, J. Fan, Y. Li, J. Huang, and J. Wang. 2014. The effect of temperature on cell growth and astaxanthin accumulation of *Haematococcus pluvialis* during a light-dark cyclic cultivation. *Bioresour. Technol.* 167:276–283. doi:10.1016/j.biortech.2014.06.030.

Wang, C., Y. Li, J. Lu, X. Deng, H. Li, and Z. Hu. 2017. Effect of overexpression of LPAAT and GPD1 on lipid synthesis and composition in green microalga *Chlamydomonas reinhardtii*. *J. Appl. Phycol.* 1–9. doi:10.1007/s10811-017-1349-2.

Wang, H., Y. Yang, A.A. Keller, X. Li, S. Feng, Y. nan Dong, and F. Li. 2016. Comparative analysis of energy intensity and carbon emissions in wastewater treatment in USA, Germany, China and South Africa. *Appl. Energy*. 184:873–881. doi:10.1016/j.apenergy.2016.07.061.

Wang, J., H. Yang, and F. Wang. 2014a. Mixotrophic cultivation of microalgae for biodiesel production: Status and prospects. *Appl. Biochem. Biotechnol.* 172:3307–3329. doi:10.1007/s12010-014-0729-1.

Wang, T., Y. Ji, Y. Wang, J. Jia, J. Li, S. Huang, D. Han, Q. Hu, W.E. Huang, and J. Xu. 2014b. Quantitative dynamics of triacylglycerol accumulation in microalgae populations at single-cell resolution revealed by Raman microspectroscopy. *Biotechnol. Biofuels*. 7:1–12. doi:10.1186/1754-6834-7-58.

Wang, T., Y. Ji, Y. Wang, J. Jia, J. Li, S. Huang, D. Han, Q. Hu, W.E. Huang, and J. Xu. 2014c. Quantitative dynamics of triacylglycerol accumulation in microalgae populations at single-cell resolution revealed by Raman microspectroscopy. *Biotechnol. Biofuels*. 7:58. doi:10.1186/1754-6834-7-58.

Warnet, X.L., A.A. Arnold, I. Marcotte, and D.E. Warschawski. 2015. In-Cell Solid-State NMR: An Emerging Technique for the Study of Biological Membranes. *Biophys. J.* 109:2461–2466. doi:10.1016/j.bpj.2015.10.041.

Warren, K.M., J.N. Mpagazehe, P.R. Leduc, and C.F. Higgs. 2014. Probing the elastic response of microalga *Scenedesmus dimorphus* in dry and aqueous environments through atomic force microscopy. *Appl. Phys. Lett.* 105:1–4. doi:10.1063/1.4898636.

Wensel, P.C., M. Bule, A. Gao, M.R. Pelaez-Samaniego, L. Yu, W. Hiscox, G.L. Helms, W.C. Davis, H. Kirchhoff, M. Garcia-Perez, and S. Chen. 2022. Biorefinery Processing of Waste to Supply Cost-Effective and Sustainable Inputs for Two-Stage Microalgal Cultivation. *Appl. Sci.* 12. doi:10.3390/app12031485.

Whitton, B.A. 2012. Ecology of cyanobacteria II: Their diversity in space and time. *Ecol. Cyanobacteria II Their Divers. Sp. Time*. 9789400738:1–760. doi:10.1007/978-94-007-3855-3.

Wu, H., J. V. Volponi, A.E. Oliver, A.N. Parikh, B.A. Simmons, and S. Singh. 2011. In vivo lipidomics using single-cell Raman spectroscopy. *Proc. Natl. Acad. Sci.* 108:3809–3814. doi:10.1073/pnas.1009043108.

Wunder, T., S.L.H. Cheng, S.K. Lai, H.Y. Li, and O. Mueller-Cajar. 2018. The phase separation underlying the pyrenoid-based microalgal Rubisco supercharger. *Nat. Commun.* 9:1–10. doi:10.1038/s41467-018-07624-w.

Xie, Y., K. Lu, X. Zhao, R. Ma, J. Chen, and S.H. Ho. 2019. Manipulating Nutritional Conditions and Salinity-Gradient Stress for Enhanced Lutein Production in Marine Microalga *Chlamydomonas* sp. *Biotechnol. J.* 14:1–28. doi:10.1002/biot.201800380.

Xiong, W., C. Gao, D. Yan, C. Wu, and Q. Wu. 2010. Double CO_2 fixation in photosynthesis-fermentation model enhances algal lipid synthesis for biodiesel production. *Bioresour. Technol.* 101:2287–2293. doi:10.1016/j.biortech.2009.11.041.

Xu, Y., I.M. Ibrahim, C.I. Wosu, A. Ben-Amotz, and P.J. Harvey. 2018. Potential of new isolates of dunaliella salina for natural β-carotene production. *Biology (Basel).* 7:1–18. doi:10.3390/biology7010014.

Yang, A., W.I. Suh, N.K. Kang, B. Lee, and Y.K. Chang. 2018. MAPK/ERK and JNK pathways regulate lipid synthesis and cell growth of *Chlamydomonas reinhardtii* under osmotic stress, respectively. *Sci. Rep.* 8:1–12. doi:10.1038/s41598-018-32216-5.

Yao, C., J. Jiang, X. Cao, Y. Liu, S. Xue, and Y. Zhang. 2018. Phosphorus Enhances Photosynthetic Storage Starch Production in a Green Microalga (Chlorophyta) *Tetraselmis subcordiformis* in Nitrogen Starvation Conditions. *J. Agric. Food Chem.* 66:10777–10787. doi:10.1021/acs.jafc.8b04798.

Yap, B.H.J., S.A. Crawford, R.R. Dagastine, P.J. Scales, and G.J.O. Martin. 2016. Nitrogen deprivation of microalgae: effect on cell size, cell wall thickness, cell strength, and resistance to mechanical disruption. *J. Ind. Microbiol. Biotechnol.* 43:1671–1680. doi:10.1007/s10295-016-1848-1.

Yin, F.-W., C.-T. Zhan, J. Huang, X.-L. Sun, L.-F. Yin, W.-L. Zheng, X. Luo, Y.-Y. Zhang, and Y.-Q. Fu. 2022. Efficient Co-production of Docosahexaenoic Acid Oil and Carotenoids in *Aurantiochytrium* sp. Using a Light Intensity Gradient Strategy. *Appl. Biochem. Biotechnol.* doi:10.1007/s12010-022-04134-w.

Yu, Z., H. Pei, L. Jiang, Q. Hou, C. Nie, and L. Zhang. 2018. Phytohormone addition coupled with nitrogen depletion almost tripled the lipid productivities in two algae. *Bioresour. Technol.* 247:904–914. doi:10.1016/j.biortech.2017.09.192.

Zhang, P., Z. Li, L. Lu, Y. Xiao, J. Liu, J. Guo, and F. Fang. 2017. Effects of stepwise nitrogen depletion on carotenoid content, fluorescence parameters and the cellular stoichiometry of *Chlorella vulgaris*. *Spectrochim. Acta - Part A Mol. Biomol. Spectrosc.* 181:30–38. doi:10.1016/j.saa.2017.03.022.

Zhao, L.S., K. Li, Q.M. Wang, X.Y. Song, H.N. Su, B. Bin Xie, X.Y. Zhang, F. Huang, X.L. Chen, B.C. Zhou, and Y.Z. Zhang. 2017. Nitrogen Starvation Impacts the Photosynthetic Performance of *Porphyridium cruentum* as Revealed by Chlorophyll a Fluorescence. *Sci. Rep.* 7. doi:10.1038/s41598-017-08428-6.

Zheng, G., F. Gu, Y. Cui, L. Lu, X. Hu, L. Wang, and Y. Wang. 2022. A microfluidic droplet array demonstrating high-throughput screening in individual lipid-producing microalgae. *Anal. Chim. Acta*. 1227:340322. doi:https://doi.org/10.1016/j.aca.2022.340322.

Zheng, X., X. Duan, X. Tu, S. Jiang, and C. Song. 2021. The fusion of microfluidics and optics for on-chip detection and characterization of microalgae. *Micromachines*. 12. doi:10.3390/mi12101137.

Zoni, V., R. Khaddaj, P. Campomanes, R. Thiam, R. Schneiter, and S. Vanni. 2020. Lipid Droplet Biogenesis is Driven by Liquid-Liquid Phase Separation. *SSRN Electron. J.* 1–30. doi:10.2139/ssrn.3526890.